UNIVERSITAT POLITÈCNICA DE CATALUNYA
BARCELONATECH
Escola Superior d'Enginyeries Industrial, Aeroespacial i Audiovisual de Terrassa

OPTIMIZATION STUDY OF FISCHER-TROPSCH GAS-TO-LIQUID (GTL) PROCESS USING ASPEN HYSYS

FINAL YEAR PROJECT (TFG)

BACHELOR'S DEGREE IN CHEMICAL ENGINEERING

MUHAMMAD FARRIS IDAHAM BIN ABDUL RASHID

DIRECTOR: MANUEL JOSE LIS ARIAS

10th JUNE 2019

CONTENTS

ABSTRACT iii
ACKNOWLEDGEMENTS iv
DECLARATION OF HONOUR v
LIST OF FIGURES vi
LIST OF TABLES vii
LIST OF ABBREVIATIONS viii
1. INTRODUCTION 1
1.1 INTRODUCTION TO FISCHER-TROPSCH TECHNOLOGY 1
1.2 PROCESS DESCRIPTION 4
1.2.1 SYNTHESIS GAS PRODUCTION 5
1.2.2 FISCHER-TROPSCH SYNTHESIS 7
1.3 SCOPE OF THE BACHELOR THESIS 12
2. OBJECTIVE 13
3. LITERATURE REVIEW 14
3.1 SYNGAS PRODUCTION UNIT 14
3.2 FISHCER-TROPSCH SYNTHESIS 15
4. MODELLING IN ASPEN HYSYS 17
4.1 AUTOTHERMAL REACTOR 19
4.2 FISCHER-TROPSCH REACTOR 21
5. EXPERIMENTAL DEVELOPMENT 23
5.1 AUTOTHERMAL RECTOR OPTIMIZATION 23
CASE 1: SYNGAS PRODUCTION UNIT WITH DIFFERENT REACTOR TYPES 23
CASE 2: STAGING OF ATR WITH DOSSIFICATION 25
5.2 FISCHER-TROPSCH REACTOR OPTIMIZATION 26
CASE 3: INFLUENCE OF COBALT CATALYST CHARACTERISTIC ON PRODUCT DISTRIBUTION 26
CASE 4: STAGING OF FTR WITH DOSSIFICATION 28
5.3 OVERALL PROCESS OPTIMIZATION 29
6. RESULTS AND DISCUSSIONS 31
6.1 RESULT OF AUTOTHERMAL REACTOR OPTIMIZATION 31
6.1.1 DISCUSSION OF AUTOTHERMAL REACTOR OPTIMIZATION 37
6.2 RESULT OF FISCHER-TROPSCH REACTOR OPTIMIZATION 39
6.2.1 DISCUSSION OF FISCHER-TROPSCH REACTOR OPTIMIZATION 43
6.3 RESULT OF OVERALL PROCESS OPTIMIZATION 45

6.3.1 DISCUSSION OF OVERALL PROCESS OPTIMIZATION 47
7. CONCLUSION 49
BIBLIOGRAPHY 50
ANNEX 52

ABSTRACT

Fischer-Tropsch (FT) technology is simply defined as the means to convert syngas to a wide range of hydrocarbon products including paraffins, olefins, oxygenates, etc. Interest in FT synthesis is increasing rapidly due to a number of factors including demand of cleaner fuel (low Sulphur, low aromatics), improvement in FT technology and the need to monetize stranded natural gas resources. Hence, there is a strong incentive to further optimize the reactions in a GTL plant so that the overall cost can be reduced.

In this study, the overall GTL process was simulated using Aspen HYSYS v8.6. The impact of different parameters on the performance of syngas unit, FTS unit and the overall process were studied. The main objective is to optimize all the main reactions involved in GTL process as well as to increase fraction of desired product. To achieve this, all the important reactions were modelled using kinetic approach obtained from literature and kinetic reactors were used.

The Auto Thermal Reactor (ATR) was modelled as CSTR and PFR in HYSYS with kinetic data given by Xu,Froment et al. and D.L Hoang et al. [11], [22]. The main objective function was to increase conversion of reaction and to produce low H_2:CO ratio in syngas. Three configurations were proposed to compare the contact model of the ATR using different reactors. CSTR was observed to produce syngas with suitable H_2:CO ratio for FTS. Staging of ATR with dossification of feed between stages was simulated however it did not show any improvement on conversion or H_2:CO ratio.

The FT reactor with cobalt based catalyst was modelled as PFR with kinetic data from Iglesia et al.[27] A few parameters were varied to observe the effect on product distribution and overall conversion. In case 3, the effect of varying void fraction in FTR was studied and the optimal value was recorded. Case 4 explored the effect of multiple stage FTR configuration. Staging of FTR recorded a higher overall conversion and product distribution also improved. An optimal FTR configuration was proposed and showed an even higher conversion compared to the multi stage FTR and an improved product distribution.

Some other process parameters were also investigated such as the inlet temperature of ATR and steam:carbon ratio in pre-reformer. Optimization of both parameters showed improvement in the syngas produced. Lower H_2:CO ratio of syngas was observed by increasing inlet temperature of ATR and reducing steam:carbon ratio. The optimal GTL plant configuration was proposed at the end of this study.

ACKNOWLEDGEMENTS

This work has been carried out at the Department of Chemical Engineering at *The Universitat Politecnica de Catalunya (UPC) - BarcelonaTECH* in Terrassa, Barcelona. I would like to take this opportunity to thank and give acknowledgements to those who have helped me complete this bachelor's thesis be it directly or indirectly.

First and foremost, I wish to express my deepest gratitude to my supervisor, Professor Manuel Jose Lis Arias for his invaluable guidance, support and encouragement during the course of this semester. I am truly grateful that he always makes time out of his busy schedule to attend to my questions and doubts. I have really enjoyed learning and working with such a complete academician like Professor Manuel and I am glad that I have learned a lot from him.

I would also like to thank all the lecturers and professors who have taught me during my four years in UPC. I have learned and grown so much since I first step into the doors of this university. The challenges I face during my bachelor's degree have certainly helped me to be stronger and wiser in life. It has been a wonderful experience completing my bachelor's degree in such a beautiful city like Barcelona.

Special thanks to all my friends here in Spain as well as back home in Malaysia. Their encouragement and support have helped me in many different ways to complete my studies. I shared so many good memories and laughter with my friends and they made my journey here in Spain easier and more enjoyable.

Many thanks to the Government of Malaysia and MARA for funding me throughout my studies in Barcelona as well as the 2 years in Malaysia where I did my A-levels. It would not have been possible without their financial support and it has surely helped me to solely focus on my studies.

Finally, this work would not have been possible without the love and support from my parents and family in Kuala Lumpur, Malaysia. Their encouragement, trust, motivation and invaluable support have made me who I am today. I will always treasure and appreciate everything they have done for me.

LIST OF FIGURES

Figure 1-1: A simplified process scheme of FTS [3] 2
Figure 1-2: GTL process block diagram [2] 3
Figure 1-3: Process flow diagram of GTL process [6] 4
Figure 1-4: Variation of product weight fraction with chain growth probability [1] 9
Figure 1-5: Multitubular fixed-bed reactor used in FTS [18] 11
Figure 3-1: syngas production unit process scheme [19] 14
Figure 3-2: Chain building of FT products [1] 16
Figure 5-1: Simulation of ATR modelled as CSTR 23
Figure 5-2: Simualtion of ATR modelled as isothermal PFR 23
Figure 5-3: Simualtion of ATR modelled as adiabatic PFR 24
Figure 5-4: Simulation of multiple stage ATR 25
Figure 5-5: HYSYS catalyst parameeters 26
Figure 5-6: Simulation of single stage FTR 27
Figure 5-7: Simulation of multi stage FTR 28
Figure 5-8: Optimal multi stage FTR configuration 29
Figure 5-9: Final GTL process configuration 30
Figure 6-1: variation of molar fraction of desired product with catalyst void fraction in FTR 40
Figure 6-2: Variation of inlet temperature of ATR with H_2:CO ratio in syngas 45
Figure 6-3: Effect of steam on H_2:CO ratio in syngas 46
Figure 6-4: Optimal GTL plant configuration 48

LIST OF TABLES

Table 1-1: Effect of changing of parameters on chain growth probability, olefin/parafin ratio, carbon deposition and methane selectivity [3] 9
Table 1-2: Ideal characteristic of FTR [18] 11
Table 3-1: Application of different catalysts used in FTS and their corressponding value of α [2] 16
Table 4-1: Molar composition of natural gas [1],[2] 17
Table 4-2: Chemical reactions in pre-reformer and corresponding enthalypy values [6] 18
Table 4-3: Feed process conditions [9],[2] 18
Table 4-4: Chemical reactions in ATR [6],[11] 19
Table 4-5: Kinetic data of reactions in ATR [11],[22] 20
Table 4-6: Chemical reactions in FTR [6] 21
Table 4-7: Kinetic data of reactions in FTR [6] 22
Table 6-1: Molar fraction data of configuration 1 31
Table 6-2: Process condition data of configuration 1 32
Table 6-3: ATR (CSTR) data 32
Table 6-4: Molar fraction data of configuration 2 33
Table 6-5: ATR (Isothermal PFR) data 33
Table 6-6 Molar fraction data of configuration 3 34
Table 6-7: ATR (Adiabatic PFR) data 34
Table 6-8: Molar fraction data of multi stage ATR 35
Table 6-9: Multi stage ATR data 35
Table 6-10: Process condition data of multi stage ATR simulation 36
Table 6-11: Summary of case study 1 37
Table 6-12: Summary of case study 2 38
Table 6-13: Variation of molar fraction of desired product with catalyst void fraction in FTR 39
Table 6-14: single stage FTR data 40
Table 6-15: Molar fraction data of multiple stage FTR simulation 41
Table 6-16: Reactor data of multiple stage FTR 42
Table 6-17: Process condition of multiple stage FTr simulation 42
Table 6-18: Summary of multi stage FTR data 44
Table 6-19: Reactor data of optimal FTR configuration 45
Table 6-20: Molar fraction of optimal ATR configuration 46

LIST OF ABBREVIATIONS

FT	-	Fischer-Tropsch
FTS	-	Fischer-Tropsh Synthesis
FTR	-	Fischer-Tropsch Reactor
GTL	-	Gas-to-Liquid
ATR	-	Auto Thermal Reactor
HTFT	-	High Temperature Fischer-Tropsch
LTFT	-	Low Temperature Fischer-Tropsch
CSTR	-	Continous Stirred Tank Reactor
PFR	-	Plug Flow Reactor
LNG	-	Liquified Natural Gas
WGS	-	Water Gas Shift
α	-	Chain Growth Pobability
ω	-	Weight Fraction
U	-	Hydrogen Usage Ratio
Φ	-	Catalyst Diffusional Coefficient
Ψ	-	Coefficient of First-order rate constant and effective diffusivity of α-olefin
χ	-	Coefficient of structural catalyst properties

1. INTRODUCTION

1.1 INTRODUCTION TO FISCHER-TROPSCH TECHNOLOGY

Historical Background

Franz Fischer and Hans Tropsch were scientists working at Kaiser Wilhem Institute for Coal Research in Germany which was founded in 1913. They wanted to produce hydrocarbon molecules using coal-derived synthesis gas (syngas) but only started to produce results in the 1920's.[1] Their intention was to fulfil the required demand for transportation fuel during the WW2 and fortunately a production of 600 000 ton/year was achieved with the use of coal gasification.[2] Fischer-Tropsch synthesis (FTS) popularity gained rapidly and was a major source of transportation fuel in Germany during WW2. However, soon after the war ended, crude oil-based fuel was economically more attractive and hence interest in FTS died down.

Since the 1980's until today, the interest in FTS is growing again mainly due to the demand for cleaner fuel. At the moment, most major oil companies are considering, developing or even operating Fischer-Tropsch Synthesis based processes to convert natural gas into liquid fuels.[3] Shell for example has a gas-to-liquid (GTL) plant in Bintulu, Malaysia which was started up in 1992 also known as Shell Middle Destillate Synthesis (SMDS) process. The currently largest operating GTL plant is the Pearl GTL plant operated by Shell and Qatar Petroleum which was commissioned in 2011. It has a total production capacity of 260,000 bbl/day; 120,000 bbl/day upstream products and 140,000 bbl/day GTL product.[4]

Fischer-Tropsch Technology

Fischer-Tropsch (FT) technology is simply defined as the means to convert syngas to a wide range of hydrocarbon products including paraffins, olefins, oxygenates, etc. Syn gas, a mixture of carbon monoxide and hydrogen, can be obtained from several sources like coal, natural gas or even biomass. In FT technology, typically natural gas is used as the source, it will then undergo reforming reactions to produce syn gas which will be fed to a FT reactor to produce a wide range of hydrocarbon products. After separation and upgrading, FTS products can be used as transportation fuels, feedstock for lubricant products and other petrochemical products. Non-fuel range products can be hydrocracked to the desired transportation fuels or be recycled to the synthesis gas generation process step. Figure 1-1 shows a simplified process scheme of the FTS.[3]

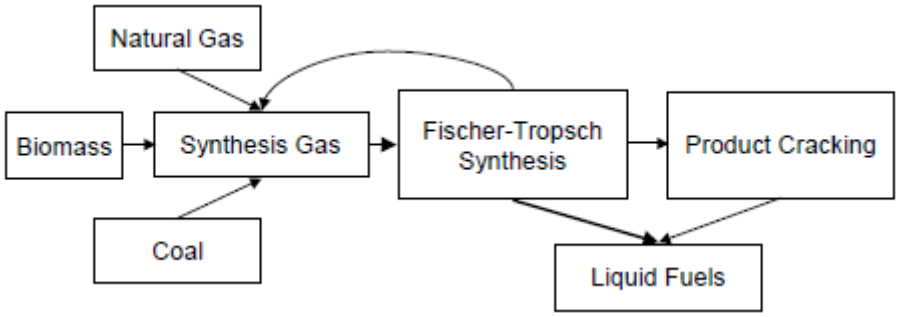

Figure 1-1: A simplified process scheme of FTS [3]

Interest in FT is increasing rapidly due to the recent improvements to the technology and also the fuel is considered a very clean fuel, with no Sulphur content, low aromatics content and lower emissions of hydrocarbons, CO, NOX and particulates upon combustion, when compared to traditional fuels.[5] In addition, GTL diesel has a superior cetane number compared to regular diesel with 70 and 45 respectively.[6] Essentially this means that GTL diesel has a higher energy density and performance than regular diesel. GTL products can be blended with traditional petroleum products making it possible to transport with current technology without the need of special tankers such as liquefied natural gas (LNG) require.[6] The realization of this process is the ideal way to monetized the stranded natural gas resources as it is not economical to transport natural gas over a very long distances. However, producing FT products may be challenging as it requires to produce syn gas as a first step. Production of syngas also has its own challenges. Hence, a closer look must be taken at the interests and challenges of the whole process which will be further discussed in the following part of this report.

Interests and challenges

The performance of the FT process depends on the composition of the streams, catalyst type, operating conditions, type of reactor, source of feedstock, etc.[1] The main challenge with this production method is the high capital cost for producing synthesis gas.[7] The synthesis gas production constitutes at least 40 % of the total investment cost for a complete GTL plant.[2] It is therefore necessary to do more research in order to find a more efficient and optimal process condition of syn gas production. These contributions could reduce the overall cost to a lower level.

Besides that, being a highly exothermic process, temperature control is vital in ensuring the process runs smoothly. High temperature will increase rate of methane production which is favorable but will also increase the chances of carbon deposition, catalyst deactivation and decreases chain growth probability of FT products which is undesirable. On the other hand, as temperature increases , the reaction rates increase and the quality of steam generated in the FT reactor improves which is desirable. [1] This means that the application of FT technology involves a number of trade-offs and compromises to get the optimal condition.

A GTL plant can be broken down to 3 main sections [1],[2],[4]:

- Syngas production
- FT synthesis
- Product upgrading

A block diagram of this process is presented in figure 1-2 below. This study will not however consider the product upgrading unit. The focus of this study is directed towards the first two sections of a GTL plant. Each of these steps involves many different chemical reactions and challenges which will be further explained and discussed in the next part of this report.

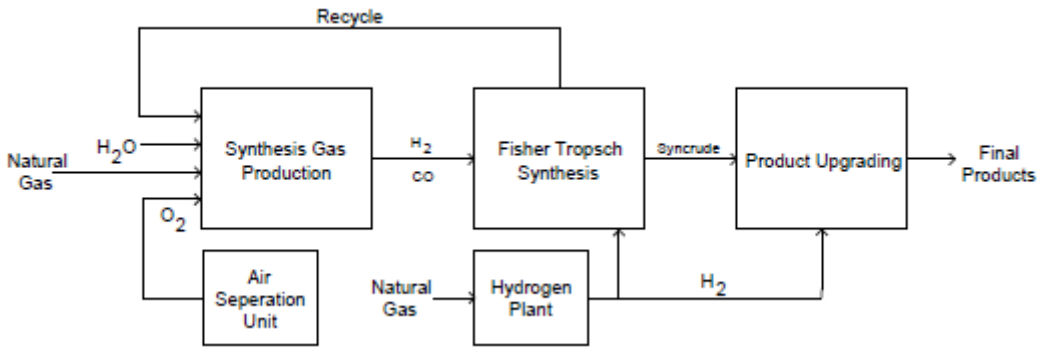

Figure 1-2: GTL process block diagram [2]

1.2 PROCESS DESCRIPTION

Figure 1-3 shows a typical process flow diagram of a GTL plant which will be modeled in this study.[6]

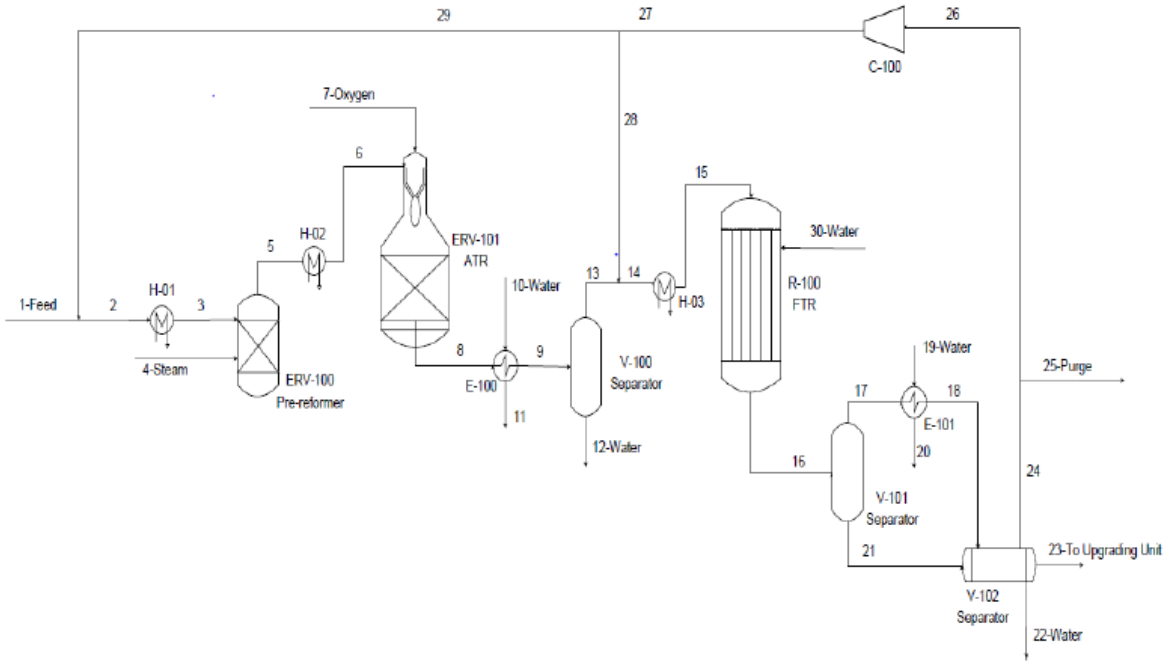

Figure 1-3: Process flow diagram of GTL process [6]

Firstly, the natural gas feed will be pre-heated and sent to the pre-reformer to crack higher hydrocarbons (C_{2+}) to a mixture of CO and H_2 by reacting it with steam before sending it to an autothermal reactor (ATR) for methane to react with oxygen to produce syngas. The syngas is now cooled to remove water before pre-heating it again and sending it to the FTR. The outlet of the FTR is called crude product which will be passed through a 3-phase separator to separate aqueous, liquid and gas streams. The liquid phase will be sent to the upgrading unit which will eventually produce GTL products. Remaining water is removed from the system and the unreacted gas will be recycled.

1.2.1 SYNTHESIS GAS PRODUCTION

We will now discuss in greater detail the syngas production unit as it is the most cost intensive part of the whole GTL process accounting up to 75% of the capital cost.[7] Hence, there is a great importance to optimize this process so that the overall GTL process is more economical.

The syngas production unit basically converts natural gas into a mixture mainly containing H_2 and CO. Typically, before natural gas feed enters syngas production unit, it is first pass through a fired heater before entering an adiabatic pre-reformer to crack higher hydrocarbons into mixture of H_2 and CO as mentioned before. This reaction usually occur at the temperature between 350-550 °C.[8]

The reactions involved in the pre-reformer can be seen below:[6]

$$C_2H_6 + 2H_2O \leftrightarrow 5H_2 + 2CO \quad (1)$$

$$C_3H_8 + 3H_2O \leftrightarrow 7H_2 + 3CO \quad (2)$$

$$C_4H_{10} + 4H_2O \leftrightarrow 9H_2 + 4CO \quad (3)$$

$$CO + 3H_2 \leftrightarrow CH_4 + H_2O \quad (4)$$

$$CO + H_2O \leftrightarrow CO_2 + H_2 \quad (5)$$

The key variable of syngas production unit is the ratio of H_2:CO produced. The optimal H_2:CO ratio depends on the FT technology. Although a usage ratio of 2:1 is implied by the FT reactions, the real usage ratio depends on the chain growth probability and product selectivity.[9] As of today, there are a few means to produce syngas with different technologies. Among them are:[2]

- Steam methane reforming
- Autothermal reforming
- Ceramic membrane reforming

In this study, we will only be discussing the autothermal reforming technology as one of the means to produce syngas from natural gas. This is because the ATR technology is regarded as the most suitable option for a large-scale safe and economic syngas production technology for a GTL process. [7][10] The ATR also produces syngas with low H_2:CO ratio which is required for the subsequent FTS while steam methane reforming produces a high H_2:CO ratio syngas.[1]

An ATR consists of a burner, a combustion chamber and a catalyst bed located inside a refractory-line steel vessel. [7] Natural gas, steam and oxygen are injected into the combustion zone where complete oxidation of methane occur at about 1900 °C where reaction (a) takes place.[2] Unconverted methane continues through the reactor and enters the reforming zone where catalytic reforming takes place, which involves reaction (b) and (c). Energy needed in the reforming reaction is supplied by the exothermic oxidation reaction, hence the name ATR because the energy needed for the endothermic reactions is supplied by itself through other exothermic reactions.

The main reactions involved in is given by the literature and are shown below: [6][11]

a) $CH_4 + 2O_2 \rightarrow CO_2 + 2H_2O$ ΔH_1= -802 kJ/mol

b) $CH_4 + H_2O \leftrightarrow CO + 3H_2$ ΔH_2= 206 kJ/mol

c) $CO + H_2O \rightarrow CO_2 + H_2$ ΔH_3= -41 kJ/mol

Reaction (a) is the complete combustion of methane producing CO_2 and water. Reactions (b) and (c) are methane reforming and water gas shift (WGS) reaction respectively.

As mentioned previously, the key variable of the syngas production unit is the H_2:CO ratio. The main reason ATR is the preferred choice is due to the low ratio of H_2:CO in the syngas produced which is suitable for the subsequent use in FTS compared to steam methane reforming which produces syngas with H_2:CO ratio of 3:1. [1] The ceramic and membrane reforming is also not favored since it is a new technology and has not been proven to be sustainable in an industrial scale but with further research and development of this technology, it could also be a good alternative to ATR in the future.

1.2.2 FISCHER-TROPSCH SYNTHESIS

The Fishcer-Tropsch process is the heart of the GTL process where syngas is converted to linear gaseous, liquid and solid hydrocarbon chains with the use of appropriate catalyst. The FTS is in principle a carbon chain building process, where CH_2 groups are attached to the carbon chain thus forming a product with long hydrocarbon chain.[10] Which reactions exactly takes place and how, is a matter of controversy, as it has been in the last century since 1930's.[12]

FT synthesis produces a wide range of products as mentioned before but the two main products are alkanes and alkenes. These reactions are highly exothermic, and to avoid an increase in temperature, which results in lighter hydrocarbons, it is important to have sufficient cooling, to secure stable reaction conditions. The total heat of reaction amounts to 25 % of the heat of combustion of the synthesis gas, and lays thereby a theoretical limit on the maximal efficiency of the FT process.[10]

This reaction involves a catalyst to be used in different types of reactor, mostly an iron or cobalt based catalyst where the reaction takes place. FTS is divided into two processes which are low or high temperature process (LTFT, HTFT) with temperatures ranging between 200-240 °C for LTFT and 300-350 °C for HTFT.[12]

If the desired products are shorter hydrocarbon chain for example, naphtha and gasoline, the most used reactor type is the gas-fluidized bed reactor operating in the HTFT temperature range with typically an iron catalyst.[2] In high temperature FTS, fixed bed reactors are not suitable to be used. This is because of the fact that carbon deposition occurs at higher temperatures which will block the reactor tubes and may poison the cobalt catalyst.[1]

On the other hand, if heavier hydrocarbons for example diesel and wax are desired, multi-tubular fixed bed reactor or slurry bubble column reactor types are more preferable which operates in the LTFT temperature range.[2] In low temperature FTS, both precipitated iron catalysts or supported cobalt catalysts may be used. Catalyst poisoning is still a risk in this process though lower compared to HTFT. This study will focus more on LTFT process and will not take into account catalyst poisoning.

As stated above, the two most used catalyst in FTS are cobalt and iron-based catalyst. Iron is cheap, but cobalt has the advantage of higher activity and longer life, though it is many times more expensive than iron catalyst.[12] On the other hand, water gas shift (WGS) reaction is active for iron catalyst but negligible for cobalt catalysts, leading to improved hydrocarbon yield.[13] Therefore, we can say that cobalt is a more suitable catalyst to be used in FTS.

The two main reactions involved in the FTS are as follow:[6]

$$CO + U\,H_2 \rightarrow \Sigma_{i=1}^{20}\,(\text{ASF Coef.})_i C_i H_{2i+2} + (\text{ASF Coef.})_{30} C_{30} H_{62} + H_2O \qquad (1)$$

$$CO + 3H_2 \leftrightarrow CH_4 + H_2O \qquad (2)$$

For the FT reaction, only paraffin products are considered in this work. Since the main product that we aim to maximize is diesel, hence the value of α is taken as 0.9. Figure 1-4 below justifies our selection of value of α = 0.9. This gives a hydrogen usage ratio,U of 2.1 given by equation 3. The stoichiometric coefficients are then calculated using the equations as outlined in a paper by Hillestad.[14]

$$U = 3 - \alpha \qquad (3)$$

$$r_{FT} = (1-\alpha)^2\,\alpha^{i-1} \qquad \text{for } C_i,\ i = 1, \ldots..20$$

$$r_{FT} = (1-\alpha)\,\alpha^{20} \qquad \text{for } C_{21\rightarrow\infty},$$

Carbon distribution in the Fischer-Tropsch synthesis is determined by the probability of chain growth on the catalyst, also called the α-value. The product distribution is often explained by a statistical distribution called Anderson, Schultz, and Flory (ASF), given by:[2]

$$\omega_i = i(1-\alpha)^2\,\alpha^{i-1}$$

where i is the number of carbon atoms, and ωi is the weight fraction of a component with length i. Probability for the chain to terminate is explained by 1-α. A graph of weight fraction of product against chain growth probability is depicted in figure 1-4:[1]

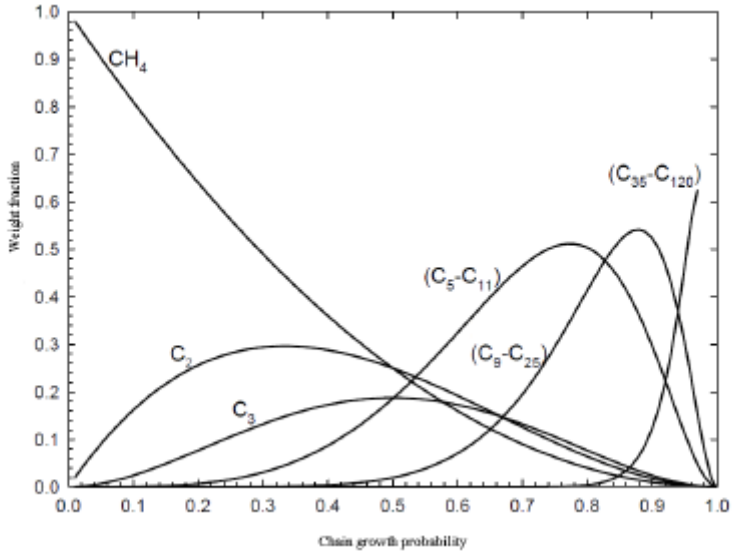

Figure 1-4: Variation of product weight fraction with chain growth probability [1]

As the graph shows, the optimum chain growth probability, which corresponds to our desired product, diesel ($C_9 - C_{25}$) is $\alpha \cong 0.9$. For cobalt catalyst, Song et al.[15] found the dependency of chain growth probability as a function of H_2:CO ratio and temperature. Low ratio H_2/CO will increase chain growth probability, and therefore the proportion of produced heavier hydrocarbons is increased. [16] The effect of temperature as explained in the previous section regarding the LTFT and HTFT also affects the chain growth probability as higher temperature causes lower chain growth probability. Other parameters that could influence chain growth probability can be summarized in table 1-1.[3] We will however not consider the formation of olefins in this study as the quantity is very small compared to the paraffin products at a specific operating condition.

Table 1-1: Effect of changing of parameters on chain growth probability, olefin/parafin ratio, carbon deposition and methane selectivity [3]

	Chain growth probability	Olefin/paraffin ratio	Carbon deposition	Methane selectivity
Temperature ↑	↓	↓	↑	↑
Pressure ↑	↑	*	*	↓
H_2/CO ratio ↑	↓	↓	↓	↑
Conversion ↑	*	↓	↑	↑
Space velocity ↑	*	↑	*	↓

There are currently four main types of reactor used in the FTS:[13], [17]

- Tubular fixed bed reactor
- Slurry phase reactor
- Circulating fluidized bed reactor
- Fluidized bed reactor

Of the four mentioned reactors, only two of them are commercially used today, the fixed bed reactor and slurry bubble column reactor. The world's largest GTL plant producing 140,000 bbl/day of petroleum liquids uses a fixed-bed reactor technology while a slurry bubble column reactor maximum production capacity as of today is about 34,000 bbl/day. Selection of type of reactor used is essential for a large-scale plant.

Multitubular reactors are widely applied to carry out exothermic reactions. They are easy to handle and to design because the parallel tubes behave very similarly. They are also easier to be scaled-up which is essential for large scale GTL plants and also helps to make the process more economical. Furthermore, there is no need for any equipment to separate the heavy wax from the catalyst particles because the liquid trickles down the catalyst. However, multitubular reactors also exhibit disadvantages such as high pressure drop and high capital cost.[18]

The second reactor type which is industrially used for FTS is the bubble column reactor with suspended catalyst. In slurry bubble columns, fine catalyst powders with dimensions of 10 to 200 µm are used.[18] Thus, the influence of internal mass transfer resistances are negligible and optimal activity and selectivity can be achieved. Internals assure efficient heat removal from the reactor that allows for a nearly isothermal operation. Even though the achievable catalyst fraction of up to 25 vol.-% is lower than in fixed bed reactors (up to 60 vol.- %), the reactor productivity of a slurry bubble column should be higher due to the enhanced catalyst utilization and the higher average reactor temperature. [18] Nevertheless, two aspects decelerated the commercialization of slurry bubble columns for FTS. Both separation of the solid catalyst from the liquid products and the scale-up of these reactors are major challenges for industrial use of slurry bubble columns.[18] Besides that, in a case of catalyst poisoning, all catalyst in a bubble column reactor would be affected compared to a fixed-bed reactor where just a portion of catalyst would be affected.

The advantages and disadvantages of both reactors mentioned can be summarized in table 1-2[18] It can be concluded that an ideal reactor concept has not been developed yet but it should have the following characteristics:[18]

- Fixed bed catalyst
- High catalyst efficiency due to short diffusion distances
- Highly efficient gas-liquid mass transfer
- Isothermal operation at highest possible temperature

Table 1-2: Ideal characteristic of FTR [18]

	Fixed bed reactor	Bubble column reactor
Pore diffusion	–	+
Catalyst content in reactor	+	–
Gas-liquid mass transfer	+	–
Isothermal behaviour	–	+
Catalyst exchange	–	+
Catalyst attrition	+	–
Need for liquid-solid separation	+	–
Scale-up	+	–
Reactor costs	–	+

Based on the reasons and discussions mentioned earlier, it has been suggested that this study will model a fixed-bed reactor for the FTS. Figure 1-5 depicts a multitubular fixed-bed reactor used in FTS process.[18]

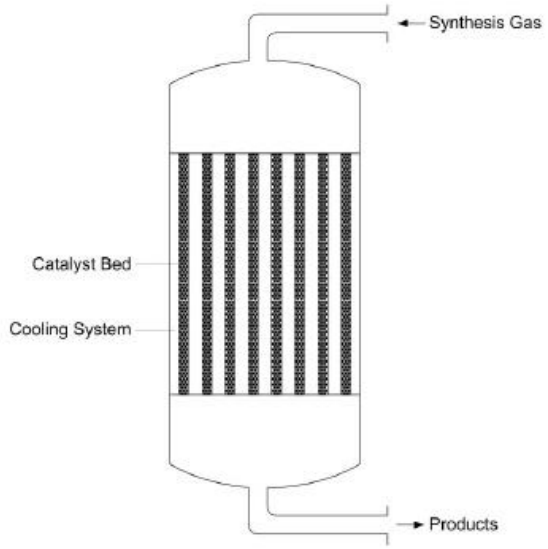

Figure 1-5: Multitubular fixed-bed reactor used in FTS [18]

1.3 SCOPE OF THE BACHELOR THESIS

A study of the GTL process covers a very wide area involving many processes and chemical reactions. We can see that there are many variables that need to be considered when aiming to optimize the GTL-FT process. In this section, the main area of study and key variables will be specified. To be able to study and optimize the GTL process, we will model and simulate the whole process using Aspen HYSYS v8.6 simulation software.

The main area of this study will be on optimization of chemical reactions in syngas production unit and FTS while also taking into account optimal condition of the process. To achieve this, we will adopt a kinetic approach to model all the main reactions in the GTL process by using Aspen HYSYS. This software will enable us to predict the behavior of the process and analyze the response of the system by changing key variables. We should also be able to understand better the chemical reactions involved in the GTL process and this will allow us to optimize the reactions and therefore increase the efficiency of the process.

As stated before, the syngas production unit and FTS will be considered while leaving out product upgrading unit in this study. For the syngas production unit, the ATR will be studied further since it is widely used in most commercial GTL plants today.

For the FT reaction, the LTFT process will be studied in depth because it produces heavier hydrocarbon chains which are valuable and easily cracked to lighter ones if required. Since products of FTS consist of various hydrocarbons, only the main product which is paraffin will be considered. The reactor of FTS that we will focus on is the fixed-bed catalytic reactor with the use of cobalt catalyst while not considering risk of catalyst deactivation.

2. OBJECTIVE

Based on the challenges faced by the industry to increase the efficiency and finding the optimal condition of the Fischer-Tropsch (FT) synthesis, this project is aimed to achieve the following objectives:

I. To model all the main reactions of the GTL process by using kinetic approach
II. To explore the possibility of staging of reactors in syngas production unit by using a kinetic approach
III. To maximize the production of longer hydrocarbon chains ($C_{13} - C_{19}$) by optimizing the reactions in both autothermal and FT reactor

In the following part of this report, a collection of works done by other researchers regarding the optimization of GTL process will be further explained and discussed. This will help us to have a better understanding of the challenges of this process and the ways to overcome them in order to achieve the stated objectives.

3. LITERATURE REVIEW

3.1 SYNGAS PRODUCTION UNIT

The syngas production unit suggested by Bakkerud [19] is shown in figure 3-1. The syngas production process includes a pre-reformer, fired heater and ATR.

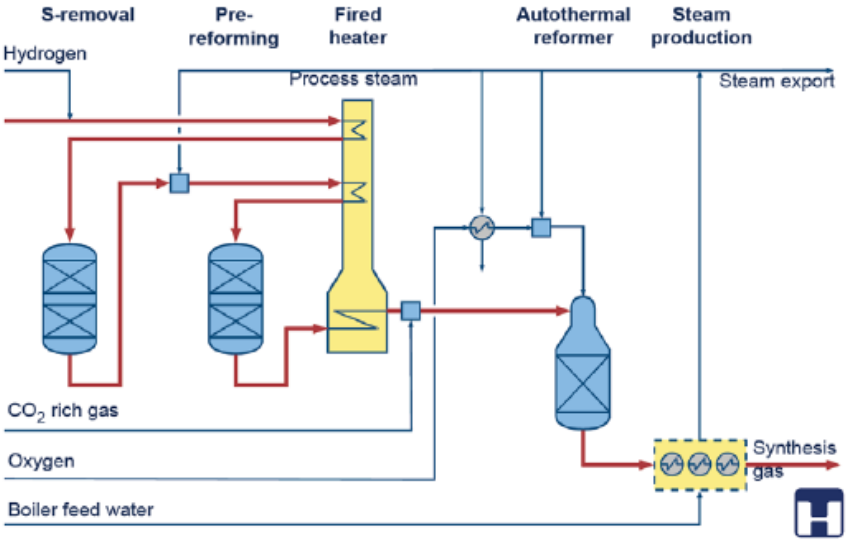

Figure 3-1: syngas production unit process scheme [19]

Typically, ATR is used to produce syngas in a GTL process as suggested by many researches in their work because it is regarded as the most economical and suitable method to produce syngas.[2], [4]–[8], [10], [20]. However, Rafiee et al. [1] has studied the combination of ATR and steam methane reforming to produce syngas called the combined reformer. He found out that by installing a steam methane reformer together with an ATR in the syngas production unit, production rate of syngas can be increased by 25.3% and total oxygen consumption will be reduced[1].

In Haldor Topsøe design (Figure 3-1), the inlet temperature to the ATR is 650°C and it is a tradeoff between available piping material and process economic considerations. The higher temperature the more oxygen is saved. The steam:carbon (S:C) ratio can affect the syngas process. If a low S:C ratio Is used, oxygen consumption in the ATR at a specific reaction temperature is also lower. But a low S:C ratio risks formation of soot. Commercial use has been proven by Haldor Topsøe with a ratio of 0.6. Even lower ratios, down to 0.2 have been reported [7] and commercialization of an ATR technology with S:C = 0.4 is expected within the near future.[1]

The H_2:CO ratio depends on the inlet composition, S:C, O_2:C, inlet temperature, etc[1], [21]. A few studies have shown that by adding or recycling rich CO_2 gas to the ATR, the equilibrium of the WGS can be shifted and lower H_2:CO ratio in syngas can be produced.[1], [20] Higher outlet temperature of

ATR can also reduce H_2:CO ratio but typically it is limited to 1030 °C due to material constraints and stability of catalyst in reactor.[1]

After scrutinizing many academic journals and theses, almost all researches modeled the ATR as a conversion or Gibbs reactor in their simulation study by assuming chemical equilibrium at the outlet of ATR. [2], [4]–[8], [10], [20] Within this study, the ATR was modeled as a kinetic reactor in Aspen HYSYS with the kinetic data obtained from Xu,Froment et al. and D.L Hoang et al.[11], [22]. The oxygen-to-carbon ratio in the ATR was adjusted to reach the temperature of 1030 °C at the outlet of the reactor as proposed by Magne Hillestad et al.[23] The effect of S:C ratio was studied further and will be optimized to produce low H_2:CO ratio in syngas.

3.2 FISHCER-TROPSCH SYNTHESIS

Most work done by researchers studying the FTS has either modeled the FT reactor as slurry bubble column reactor or multitubular fixed bed reactor as they are the most widely used commercially today. The majority of research also focus on LTFT process instead of HTFT because of the more valuable products in LTFT.

A number of ways have been developed to optimize the FTS to increase its efficiency. Works by Rafiee et al.[1], K.Moen et al.[2], C.Maretto et al.[24] and Magne Hillestad et al.[25] have all suggested that staging of the FTR could increase the conversion and improve efficiency. This method was first proposed by M.Hillestad[26] with kinetic data from Iglesia et al. based on cobalt catalyst.[27] They argued that with staging of FTR, mass fraction of desired product and CO conversion improves significantly. Rafiee [1]suggested that optimal mixing structure of a 2-stage FTS is CSTR for the first stage and PFR for the second. He stated that the CSTR will level out the temperature peak before entering the second stage.

K.Moen [2] suggested that extra H_2 feed to be injected between stages of the FTR so that the ratio of H_2:CO remains constant between each stage as he noted that H_2 is used up more than its stoichiometric coefficient compared to CO. He also argued that by removing water after every stage will increase the conversion in the FTR even higher, stating the fact that the residence time will increase as the feed is not diluted with water. However, he noted that this involves a higher capital cost as the need for more 3-phase separators, coolers and heaters and also causing the increase in utility cost. K.Moen [2] concluded that the best configuration of the FTS would be a 3 stage FTR and some of the steam is replaced by CO_2 which would result in higher energy and carbon efficiency.

The product distribution of the FTS synthesis can be explained by the ASF distribution as suggested by many researchers[1], [2], [6]. As the FTS in principle a chain building process, the chain growth probability according to ASF distribution theory can be called α and the chain termination probability is called 1-α. The figure 3-2 depicts the chain building process.[1]

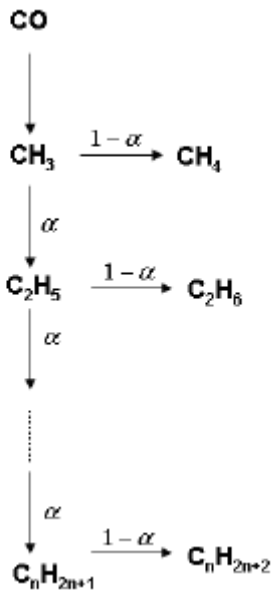

Figure 3-2: Chain building of FT products [1]

α depends on a number of things including temperature and type of catalyst used. Table 3-1 shows the typical value of α for different catalysts and products. [2]

Table 3-1: Application of different catalysts used in FTS and their corressponding value of α [2]

Catalyst	α	Main product
Nickel	Low	Methane
Iron	0.65-0.70	Gasoline
Cobalt	0.75-0.85	Waxes

In this study, the FTS synthesis was modeled as a PFR in Aspen HYSYS as the idea is to simulate it as a multitubular fixed bed reactor. K.Moen[2] and Otaraku et al.[6] also did the same by modelling the FTR as PFR in their simulation study. However, O.Kristian [8] modeled the FTR as a CSTR citing that he models the reactor as a slurry bubble column reactor. Cobalt catalyst used will be modeled in the simulation and the kinetics data is given by Iglesia et al.[27] Staging of FTR as proposed by Hillestad[26] and studied by Rafiee[1] was investigated and optimized while finding the optimal configuration as suggested by K.Moen[2] in his study.

4. MODELLING IN ASPEN HYSYS

In this study, the GTL plant was simulated using Aspen HYSYS© version 8.6 simulation software. In setting up the model, the fluid package chosen was Peng-Robinson (Equation Of State) because this EOS should be able to accurately calculate all fluid properties of natural gas processes.[8] This fluid package was also selected because it has an accurate equilibrium calculation for systems consisting of mainly hydrocarbons.[2] Hydrocarbon components with four or more C-atoms were added as n-type hydrocarbons and $C_{21\rightarrow\infty}$ were modelled as C_{30} due to their similarities in properties. The reactions were added in sets for the three main unit operations namely the pre-reformer, ATR and FT reactor.

The main feedstock for this GTL plant simulation is natural gas which consist mainly of methane. Other raw materials needed in this process are pure oxygen and steam. Table 4.1 shows the molar composition of natural gas feedstock.[1], [2]

Table 4-1: Molar composition of natural gas [1],[2]

Composition	Mol fractions
Methane	0.95
Ethane	0.02
Propane	0.015
i-Butane	0.01
i-Pentane	0.005

All the heat exchangers in figure 1-3 were modelled as heaters or coolers while any fired heaters were modelled as heaters. This was done to simplify the simulation.

Natural gas enters the system at 40 °C and 3000 kPa. Before entering the pre-reformer, it was heated to 455 °C, as it is in the common range for the inlet temperature of the pre-reformer. The heated natural gas was then fed into the pre-reformer together with steam which has a temperature of 252°C. The pre-reformer converts heavy hydrocarbons (C_{2+}) into a mixture of CO and H_2. This will help avoid formation of carbon in the ATR. The reactions modelled in the pre-reformer can be seen in table 4.2 and their corresponding enthalpy of reaction.[6]

Table 4-2: Chemical reactions in pre-reformer and corresponding enthalypy values [6]

Reaction	$\Delta_{rxn} H^{\circ}_{298}$ [kJ/mol]
$C_2H_6 + 2H_2O \leftrightarrow 5H_2 + 2CO$	350
$C_3H_8 + 3H_2O \leftrightarrow 7H_2 + 3CO$	500
$C_4H_{10} + 4H_2O \leftrightarrow 9H_2 + 4CO$	650
$CO + 3H_2 \leftrightarrow CH_4 + H_2O$	-210
$CO + H_2O \leftrightarrow CO_2 + H_2$	-41

The pre-reformer was simulated as an equilibrium reactor and the reactions as an equilibrium set. Since all the reactions modelled in the reaction set are equilibrium reactions and the temperature inside the reactor is high, all higher hydrocarbons were completely converted. Therefore, it is acceptable to use an equilibrium reactor.

The outlet of the pre-reformer reactor which comprises mainly of natural gas and a small amount of H_2 and CO were fed into the ATR together with pure oxygen. This part will be discussed further in the next subsection. Table 4-3 summarizes the feed conditions of the main feedstocks in this process. They are based on values given by in an article on GTL optimization by Panahi et al and Kristoffer Moen et al.[9][2]

Table 4-3: Feed process conditions [9],[2]

Input	T(°C)	Pressure (kPa)	Molar flow (kmol/h)
Natural Gas	40	3000	22,000
Steam	252	4045	11,000
Oxygen	200	3000	13,000

4.1 AUTOTHERMAL REACTOR

In the ATR is where syngas was produced from natural gas and oxygen which was fed together into the ATR. The three main reactions and their corresponding enthalpy of reaction is listed in table 4-3.[6][11]

Table 4-4: Chemical reactions in ATR [6],[11]

Reaction	$\Delta_{rxn} H^{\circ}_{298}$ [kJ/mol]
1) $CH_4 + 2O_2 \rightarrow CO_2 + 2H_2O$	-802
2) $CH_4 + H_2O \leftrightarrow CO + 3H_2$	206
3) $CO + H_2O \rightarrow CO_2 + H_2$	-41

The ATR was modelled as a kinetic reactor with heterogenous catalyst. The reaction set for ATR was consequently also modelled as kinetic reactions. The kinetic data was obtained from J. Xu et al and D.L Hoang et al[11], [22]. The kinetic data needed to model in Aspen HYSYS is shown in the following table 4-4. The kinetic rate equations for reaction (1)-(3) are shown below.[11]

$$R_1 = \frac{k_1 p_{CH4}\, p_{O2}^{\frac{1}{2}}}{\left(1 + K_{CH4}^{C}\, p_{CH4} + K_{O2}^{C}\, p_{O2}^{\frac{1}{2}}\right)^2} \qquad (1)$$

$$R_2 = \frac{k_2}{p_{H2}^{2.5}} \left(p_{CH4} p_{H2O} - \frac{(p_{H2}^3 p_{CO})}{K_{e^2}} \right) * \frac{1}{Q_r^2} \qquad (2)$$

$$R_3 = \frac{k_3}{p_{H2}} \left(p_{CO} p_{H2O} - \frac{(p_{H2} p_{CO2})}{K_{e^3}} \right) * \frac{1}{Q_r^2} \qquad (3)$$

$$Q_r = 1 + K_{CO} p_{CO} + K_{H2} p_{H2} + K_{CH4} p_{CH4} + \frac{K_{H2O}\, p_{H2O}}{p_{H2}} \qquad (4)$$

where *R*j (kmol/kg cat h) is the rate of reaction j (j = reactions1–3); *p*XCH_4, *p*O_2, etc. are, respectively, partial pressures of gas species CH_4, O_2, etc., *k*j = *k*oj × *e(−Ej)/RT* is the kinetic rate constant of reactions j (j = reactions1–3).

Table 4-5: Kinetic data of reactions in ATR [11],[22]

Reaction	k_{oj} (kmol/ kg cat h)	E_j (kJ/mol)
1	$5.852 * 10^{17}\ bar^{-1.5}$	204.00
2	$54.225 * 10^{15}\ bar^{0.5}$	240.10
3	$1.955 * 10^{6}\ bar^{-1}$	67.13

The inlet temperature was set at 675 °C by means of a cooler. This temperature could have been set lower but that would cause the Air Separating Unit to be more expensive. Furthermore, Inlet temperature should not exceed this temperature due to material constraints.[28] As the reactions in the ATR is highly exothermic, a maximum outlet temperature was kept constant at 1030 °C by adjusting the flow rate of oxygen. This was done by the adjust block available on Aspen HYSYS software. By doing this, the reactor was modelled as an adiabatic reactor. At 1030 °C, the reactions in ATR was assured to be soot free.

A heat exchanger was connected downstream of the ATR to bring the temperature of the syngas down to 38 °C so that the steam generated in the ATR is condensed to water that can be separated out before the FT-reaction, thus reducing the volume flow and hence the reactor size.[6] The next step of the GTL process which is the FTS is explained in the next subsection.

4.2 FISCHER-TROPSCH REACTOR

The FTR is the most important unit in a GTL plant as it produces the main GTL products which consist of diesel, wax, etc. LTFT process was modelled in this study with temperature range between 200-240°C. Details of the reactions inside the FTR is described in table 4-5 below.

Table 4-6: Chemical reactions in FTR [6]

Reaction	$\Delta_{rxn} H^{\circ}_{298}$ [kJ/mol]
$\mathbf{CO + 2.1\ H_2 \rightarrow \Sigma_{i=1}^{20}\ (ASF\ Coef.)_i C_i H_{2i+2} + (ASF\ Coef.)_{30} C_{30} H_{62} + H_2O}$	-160
$\mathbf{CO + 3H_2 \leftrightarrow CH_4 + H_2O}$	-210

The complete chemical equation that was introduced in Aspen HYSYS to simulate the FT reaction is shown below. The calculation of the stoichiometric coefficient was done as explained in section 1.2.2.

CO + 2.1H_2 **→ 0.01**CH_4 **+ 0.009C2H6 + 0.008C3H8 + 0.007C4H10 + 0.007C5H12 + 0.006C6H14 + 0.005C7H16 + 0.005C8H18 + 0.004C9**H_2**0 + 0.004C10**H_2**2 + 0.003C11**H_2**4 + 0.003C12**H_2**6 + 0.003C13**H_2**8 + 0.003C14H30 + 0.002C15H32 + 0.002C16H34 + 0.002C17H36 + 0.002C18H38 + 0.002C19H40 + 0.001C20H42+ 0.012C30H62 +** H_2**O**

The FTR was modelled as a plug flow reactor (PFR) in Aspen HYSYS as this being the flow pattern that most resembles that of a multitubular fixed bed reactor. The volume of reactor was taken as 1000 m3 as starting volume and the optimum volume was investigated. The FT reaction was defined as a kinetic reaction with heterogenous catalyst and it included both the FT reaction and methanation reaction.

The stoichiometric coefficients for the FT reactions were modelled based on the ASF-distribution and the kinetics was implemented by the use of Iglesias rate of reactions. The Iglesias rate expressions in the form needed in Aspen HYSYS is given in Equation (5) and (6) while the values for A, E, n and the various component exponents for the respective equations is given in Table 4-6.[6]

$$r_{CH4} = \frac{k_1 p_{H2} p_{CO}^{0.05}}{1+(K_1 p_{CO})} \quad (5)$$

$$r_{CO} = \frac{k_2 p_{H2}^{0.6} p_{CO}^{0.65}}{1+(K_1 p_{CO})} \quad (6)$$

Table 4-7: Kinetic data of reactions in FTR [6]

Reaction	A	-E	Exponent PH_2	Exponent PCO		n
				Numerator	Denominator	
rCH_4						
k1	8.80E-06	37326	1	0.05	-	-
K1	1.10E-12	-68401.5	-	-	1	1
rCO						
k2	1.60E-05	37326	0.6	0.65	-	-
K1	1.10E-12	-68401.5	-	-	1	1

The syngas entering the FTR was preheated to 210 °C by passing it through a heater. This temperature coincides with the temperature range of LTFT process. The reactor was modelled as an isothermal reactor by fixing the outlet temperature at 220 °C and attaching an energy stream to the reactor in Aspen HYSYS. This was done so that the reaction temperature is controlled and stays within the temperature range of LTFT process.

It is only possible to have one exit stream when using PFR in Aspen HYSYS. Hence, to separate the products, a 3-phase separator was placed downstream of the FTR. The gaseous product from the FTR was first cooled down to 38 °C before entering the 3-phase separator. The outlets of the separator consist of unreacted gas, unrefined product and water. The unrefined product would be sent to a product upgrading unit before it can be used commercially.

The increase in conversion of the desired product is one the main objective of this study. To achieve this, the reaction in FTR was optimized through different methods and a number of case studies were carried out. In the next chapter, the case studies that has been carried out to meet the objectives of this study will be explained and discussed in great detail.

5. EXPERIMENTAL DEVELOPMENT

5.1 AUTOTHERMAL RECTOR OPTIMIZATION

CASE 1: SYNGAS PRODUCTION UNIT WITH DIFFERENT REACTOR TYPES

In case 1, the effect of different reactor types in syngas production unit was studied and simulated in Aspen HYSYS. The main objective function to be optimized is the H_2:CO ratio which should be around 2. CSTR and PFR were used to model the ATR in the syngas production unit. Firstly, the syngas production unit was simulated using CSTR and the results were recorded. Then, the CSTR was replaced by the PFR and simulated again. The performance and results of both of the reactors were compared to each other. This was done to study the optimal contact model of the ATR to produce syngas with H_2:CO≅2. The flowsheet of the simulated syngas process configuration in HYSYS with CSTR and PFR is shown in figure 5-1 and figure 5-2 respectively.

Configuration 1

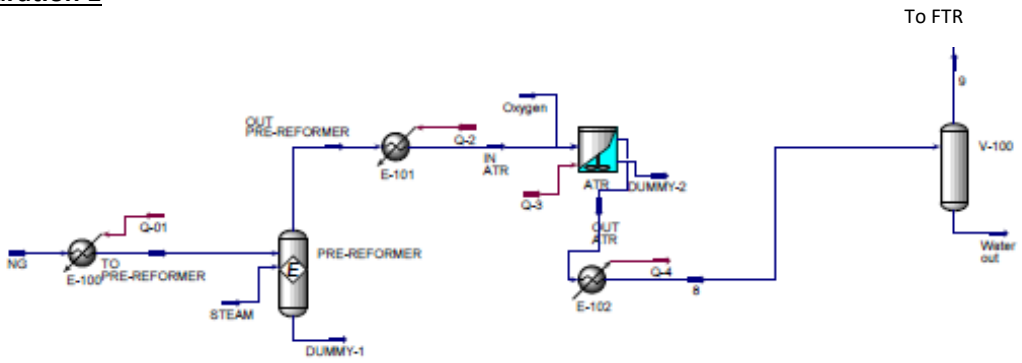

Figure 5-1: Simulation of ATR modelled as CSTR

Configuration 2

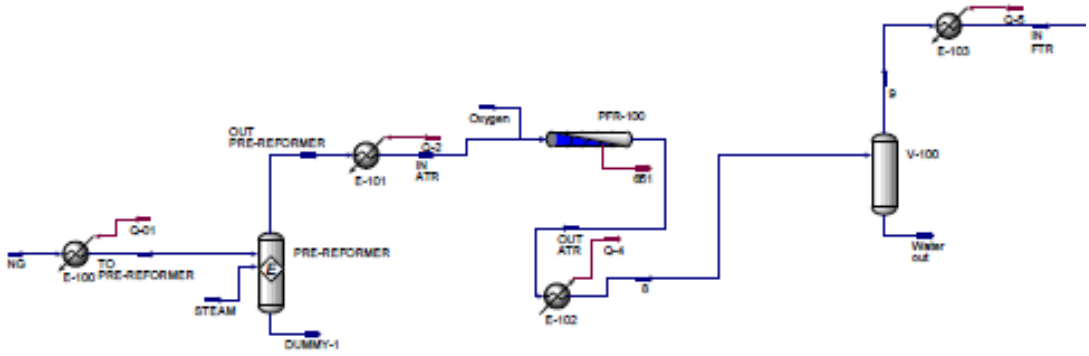

Figure 5-2: Simualtion of ATR modelled as isothermal PFR

Both configurations in figure 5-1 and 5-2 were simulated with the same kinetic reaction set and kinetic data. The operating condition was also set to be constant to facilitate comparison of the reactors. All reaction details and operating condition can be found in section 4.1.

Another configuration was also simulated as shown in figure 5-3. This configuration is similar to the figure 5-2 except that the ATR was modelled as an adiabatic reactor by adjusting the oxygen flow rate using the adjust block so that the outlet temperature of the ATR remains constant at 1030 °C. Configuration 3 were compared to configuration 2 to study the effect of adiabatic and isothermal PFR on overall conversion. All three configurations were simulated with the same reaction set and process condition to facilitate comparisons.

Configuration 3

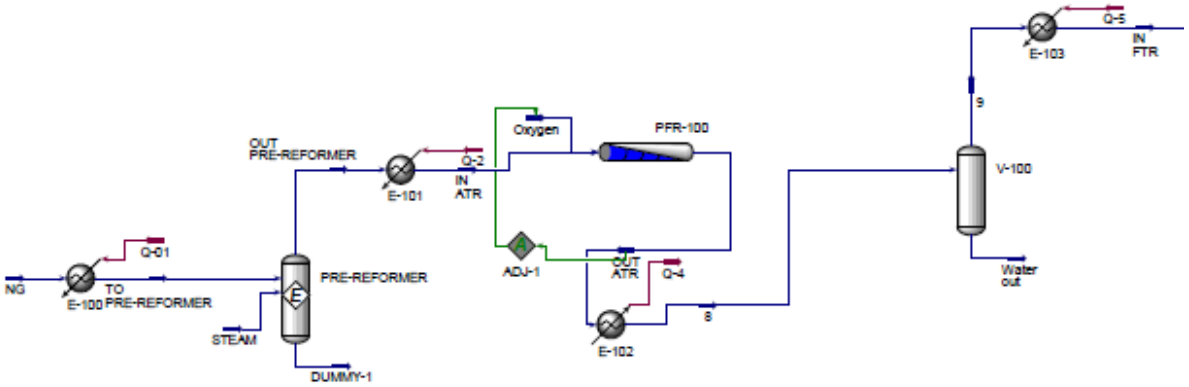

Figure 5-3: Simualtion of ATR modelled as adiabatic PFR

The pressure drop in the heaters and coolers were set to be 100 kPa whereas in the ATR it was set to 200 kPa. The results of all 3 configurations were recorded and compared which can be seen in the next chapter.

CASE 2: STAGING OF ATR WITH DOSSIFICATION

In this case, the effect of staging of ATR in the syngas production unit was investigated. In this configuration, multiple ATRs were placed in series and pure oxygen was injected into the 2nd and subsequent reactors. This was done to ensure a constant CH_4:O_2 ratio in all the ATRs since it was observed that the outlet of each ATR has a higher CH_4:O_2 ratio compared to the inlet. The objective function was to obtain syngas with H_2:CO≅2 and to increase conversion. The flowsheet of case 2 configuration can be seen in figure 5-4. In case 2, the steam:carbon ratio was reduced to 0.5 based on the result of case 1 so that it produces syngas with lower H_2:CO ratio.

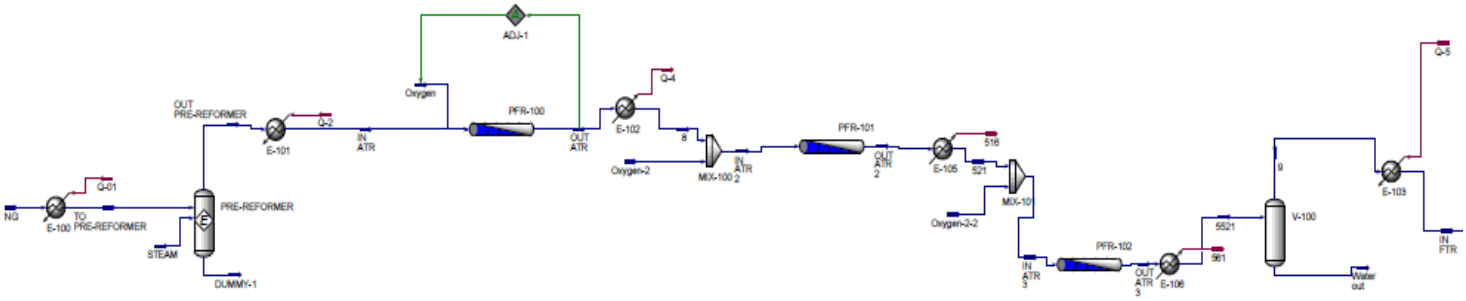

Figure 5-4: Simulation of multiple stage ATR

As shown in figure 5-4 above, the case 2 configuration was simulated with multiple PFRs modelled as ATR with multiple stages. The total volume of the reactors was kept constant in all configurations. This is to ensure that the volume of reactor does not affect the conversion. All three PFRs was attached with the same reaction set and the operation conditions was also kept constant in all configurations. Between each PFR, a cooler was placed to cool down the reactant to the reaction temperature which is 675 °C.

In the first ATR, the reactor was modelled as adiabatic reactor similar to the configuration shown in figure 5-3. In the subsequent reactors, they were modelled as isothermal reactors with the same CH_4:O_2 ratio used in the first reactor. This was done because HYSYS takes a long time to simulate all three reactors as adiabatic reactors with adjust blocks. This however would not affect our result since in each reactor, the inlet composition of reactants remains constant with the help of oxygen dossification. The result of case 2 configuration was recorded and will be discussed in the next chapter.

5.2 FISCHER-TROPSCH REACTOR OPTIMIZATION

CASE 3: INFLUENCE OF COBALT CATALYST CHARACTERISTIC ON PRODUCT DISTRIBUTION

The next case study that was conducted involves the FTR which produces hydrocarbon products. In case 3, the influence of variation of catalyst characteristic in FTR on product distribution was investigated. Among the catalyst characteristics that were studied are:

- Void fraction
- Particle sphericity
- Particle diameter
- Solid density

This was done using Aspen HYSYS simulation software. HYSYS permits the variation of catalyst parameters under the reactions tab as shown in figure 5-5 below. The void fraction parameter can be changed in the rating tab of the PFR.

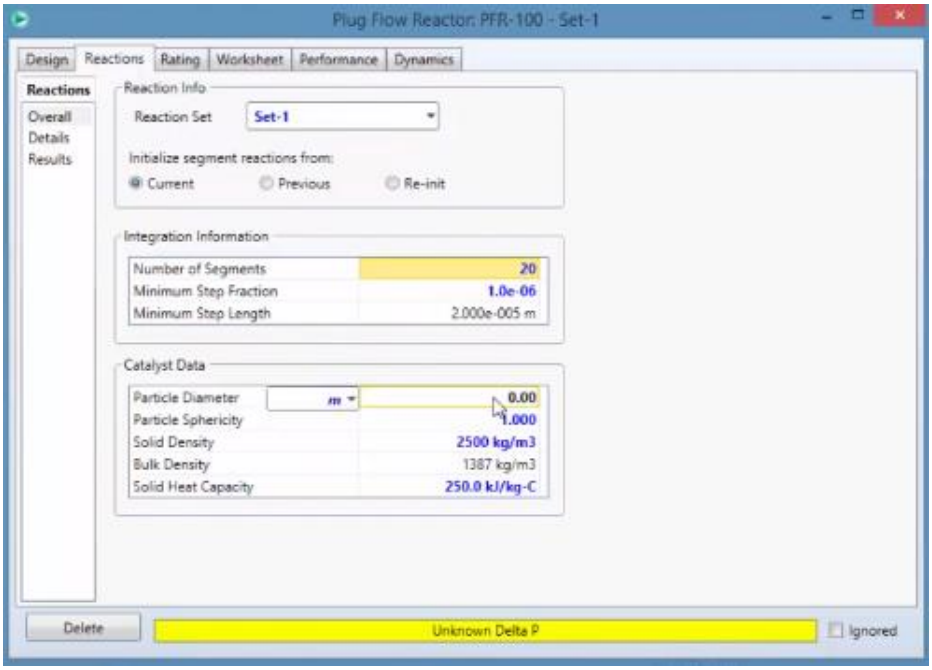

Figure 5-5: HYSYS catalyst parameeters

The objective of this case study is to maximize the production of middle distillate as it is our desired product while also taking into account overall conversion. The hydrocarbon chain the we aim to maximize is in the range of $C_{11} - C_{19}$. Only one parameter was changed at a time to observe the effect on product distribution.

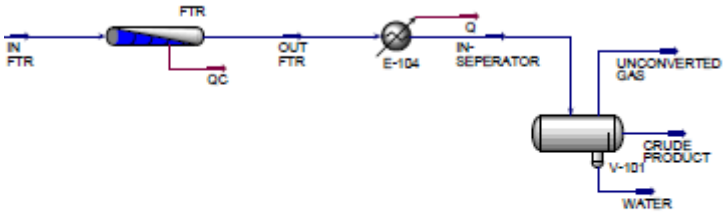

Figure 5-6: Simulation of single stage FTR

The flowsheet of this case study simulated in Aspen HYSYS can be seen in figure 5-6. The effect of product distribution was observed by comparing the composition data of the "crude product" stream as shown in the figure above. A few graphs were plotted showing the variation of product distribution with respect to change in catalyst parameter. The result of this case study will be shown in the next chapter.

As seen in the figure above, a single stage FTR was simulated. The result of this case study will be compared with the next case study which involves multiple stage FTR. Total volume of reactor will be kept constant and optimum void fraction will be used in all FTR.

CASE 4: STAGING OF FTR WITH DOSSIFICATION

The next case study that was conducted is the effect of staging of FTR to increase conversion and improve product distribution. The configuration proposed for this case study is somewhat similar to case 2: Staging of ATR but with multiple PFRs arranged in series and dossified with pure hydrogen. The flowsheet as simulated in HYSYS is shown in figure 5-7.

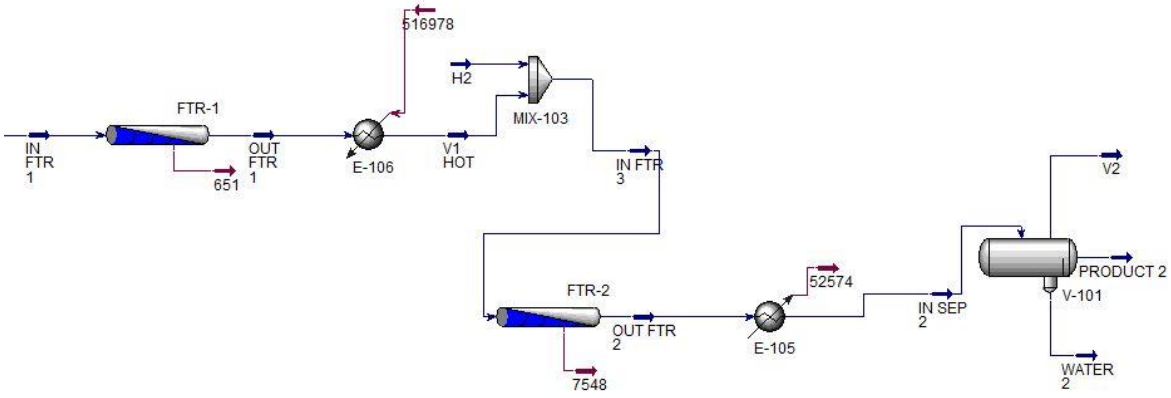

Figure 5-7: Simulation of multi stage FTR

The syngas produced from the ATR passed through a heater to heat it up to 210 °C before being fed to the FTR. The FTR was modelled as an isothermal reactor as the outlet temperature was set to 220°C. To model this in HYSYS, an energy stream was attached to the PFR. The outlet of the first ATR was then cooled to 210°C by a cooler and then dossified with pure H_2 stream in a stream mixer. This was done to ensure constant H_2:CO ratio of reactants at the entry of each reactor since it was observed that H_2:CO ratio decreases at the exit of each reactor. This shows that the consumption of H_2 is slightly higher than its stoichiometric coefficient.

At the exit of the last FTR, the exit stream was cooled to 30°C to condensed the vapor and was passed through a 3-phase separator. The 3-phase separator separated the aqueous, liquid and gas streams from each other. The aqueous stream which consisted of H_20 was discharged and the unreacted gas stream was purged. The gas stream could also be recycled into the system but it was not considered in this study. The liquid phase which consisted of the main product was sent to the product upgrading unit.

5.3 OVERALL PROCESS OPTIMIZATION

After studying all the case studies proposed as mentioned before, an optimum configuration was proposed. The optimal configuration has taken into account the optimization of both ATR and FTR which includes staging of reactors, optimal reactor type and optimal catalyst parameters. Furthermore, a few optimizations of operation condition have also been proposed. Among the proposed optimization of operation condition are:

I. Variation of inlet temperature of ATR to improve H_2:CO ratio
II. Separation product and by-product after each stage of FTR
III. Single stage ATR
IV. Optimum Steam:Carbon ratio

For the first proposed optimization, the inlet temperature was varied by changing the inlet temperature of pure oxygen. The main parameter to be optimized is the H_2:CO ratio. The objective is to obtain H_2:CO≅2 by varying the inlet temperature. A graph was plotted to show the effect of inlet temperature in ATR on the H_2:CO ratio of syngas. The result is shown in the next chapter.

The next proposed optimization is separating the product and by-product between each stage of the FTR. The objective function is to increase conversion and improve product distribution so that more desired product is formed. The process flow diagram as simulated in HYSYS can be seen in figure 5-8.

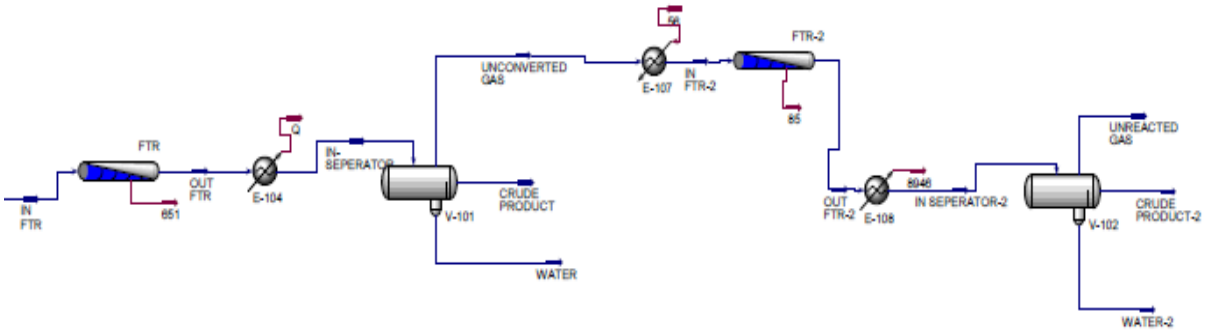

Figure 5-8: Optimal multi stage FTR configuration

The exit of the first FTR is cooled before entering a 3-phase separator. Here, the separation of unconverted syngas from crude product and water takes place. Only the unconverted gas is passed through the second FTR for the subsequent FT reaction. This configuration should increase the residence time and decrease duty of heater. However, this configuration will also cause higher capital cost as extra 3-phase separators and heaters are needed. The effect of separation of product, by-product from unreacted syngas on overall conversion was studied and the results were recorded. The final configuration which was determined as the optimal configuration is shown in figure 5-9 below.

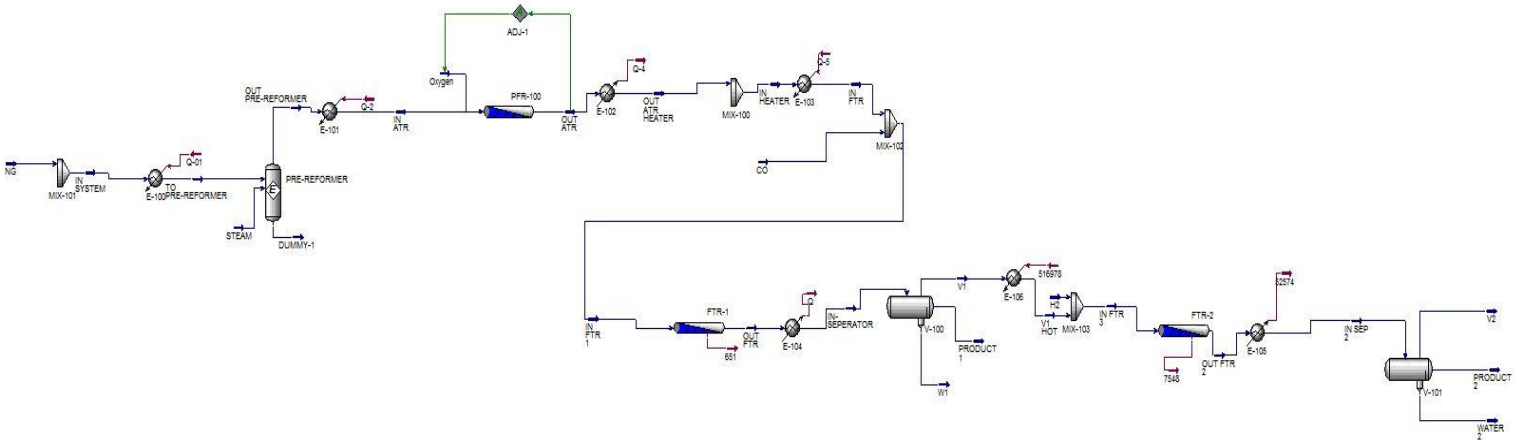

Figure 5-9: Final GTL process configuration

The results of all the proposed configurations and case studies are presented in the next chapter. A thorough analysis was done and the discussions are presented in chapter 6 of this thesis which can be found in the next page.

6. RESULTS AND DISCUSSIONS

6.1 RESULT OF AUTOTHERMAL REACTOR OPTIMIZATION

Case 1: Syngas production unit with different reactor types

The case 1 configuration was simulated in Aspen HYSYS as described in section 5.1. As mentioned in said section, there are 3 different configurations which was investigated. Firstly, we will compare configuration 1 to configuration 2. This comparison is done to observe the effect of different reactor modelled as the ATR on H_2:CO ratio. In this case, the ATR in configuration 1 was modelled as CSTR while in configuration 2 it was modelled as PFR. Both reactors have the same volume. We will now observe the result of the simulation of these two configurations. Among the parameters to be considered are:

- H_2:CO ratio
- Overall conversion

Configuration 1

Table 6-1 shows mole fraction composition of all relevant streams which involve the ATR.

Table 6-1: Molar fraction data of configuration 1

	NG	TO PRE-REFORMER	DUMMY-1	OUT PRE-REFORMER	STEAM	IN ATR	Oxygen	DUMMY-2	OUT ATR
Comp Mole Frac (H_2O)	0	0	0.333	0.333	1	0.333	0	0.207	0.207
Comp Mole Frac (Oxygen)	0	0	0.000	0.000	0	0.000	1	0.006	0.006
Comp Mole Frac (Methane)	0.95	0.95	0.611	0.611	0	0.611	0	0.000	0.000
Comp Mole Frac (Ethane)	0.02	0.02	0.000	0.000	0	0.000	0	0.000	0.000
Comp Mole Frac (Propane)	0.015	0.015	0.000	0.000	0	0.000	0	0.000	0.000
Comp Mole Frac (i-Butane)	0.01	0.01	0.000	0.000	0	0.000	0	0.000	0.000
Comp Mole Frac (i-Pentane)	0.005	0.005	0.003	0.003	0	0.003	0	0.001	0.001
Comp Mole Frac (CO)	0	0	0.000	0.000	0	0.000	0	0.282	0.282
Comp Mole Frac (Hydrogen)	0	0	0.033	0.033	0	0.033	0	0.503	0.503

The green box indicated in table 6-1 highlights the mole fraction of CO and Hydrogen gas in the outlet stream of the ATR. The ratio of H_2:CO which was determined based on this result is 1.8. It is also necessary to look into the process conditions of the inlet and outlet streams of the system to determine energy usage and the yields of the products of the simulated configuration. In table 6-2, all the process conditions of all relevant streams are specified. The process condition of all three configurations is the same. Reactor data is also shown in table 6-3.

Table 6-2: Process condition data of configuration 1

	Unit	NG	TO PRE-REFORMER	OUT PRE-REFORMER	STEAM	IN ATR	Oxygen	OUT ATR
Vapour Fraction		1	1	1	1	1	1	1
Temperature	*C*	40	455	388	252	675	200	1030
Pressure	*kPa*	3000	2900	2900	4045	2800	3000	2600
Molar Flow	*kgmole/h*	22000	22000	34488	11000	34488	12038	80271
Mass Flow	*kg/h*	383803	383803	581970	198166	581970	385204	967169
Liquid Volume Flow	*m3/h*	1221	1221	1486	199	1486	339	2682
Heat Flow	*kJ/h*	-1.68E+09	-1.21E+09	-3.80E+09	-2.60E+09	-3.24E+09	6.20E+07	-3.18E+09

Table 6-3: ATR (CSTR) data

ATR (CSTR)		
Vessel Temperature	1030	°C
Vessel Pressure	2800	kPa
Vapor Molar Flow	3.12E+04	kgmole/h
Heat Flow	-9.81E+07	kJ/h
Act.% Conversion_1	100	
Act.% Conversion_2	100	
Act.% Conversion _3	29.52	

Configuration 2

The ATR was modelled as an isothermal PFR in configuration 2 as stated earlier. Table 6-4 demonstrates the molar compositions of the relevant streams.

Table 6-4: Molar fraction data of configuration 2

	NG	TO PRE-REFORMER	OUT PRE-REFORMER	STEAM	IN ATR	Oxygen	OUT ATR
Comp Mole Frac (H_2O)	0.000	0.000	0.333	1.000	0.333	0.000	0.0000
Comp Mole Frac (Oxygen)	0.000	0.000	0.000	0.000	0.000	1.000	0.0000
Comp Mole Frac (Methane)	0.950	0.950	0.611	0.000	0.611	0.000	0.0243
Comp Mole Frac (Ethane)	0.020	0.020	0.000	0.000	0.000	0.000	0.0000
Comp Mole Frac (Propane)	0.015	0.015	0.000	0.000	0.000	0.000	0.0000
Comp Mole Frac (i-Butane)	0.010	0.010	0.000	0.000	0.000	0.000	0.0000
Comp Mole Frac (i-Pentane)	0.005	0.005	0.003	0.000	0.003	0.000	0.0014
Comp Mole Frac (CO)	0.000	0.000	0.000	0.000	0.000	0.000	0.0170
Comp Mole Frac (Hydrogen)	0.000	0.000	0.033	0.000	0.033	0.000	0.7008

Operating condition of all the mentioned streams is similar to configuration 1 which has been specified in table 6-2. The reactor data of the isothermal PFR can be seen below in table 6-5.

Table 6-5: ATR (Isothermal PFR) data

ATR (Isothermal PFR)		
Vessel Temperature	1030	°C
Vessel Pressure	2800	kPa
Vapor Molar Flow	3.12E+04	kgmole/h
Act.% Conversion_1	2.7E+05	
Act.% Conversion_2	60.86	
Act.% Conversion _3	30.70	

Configuration 3

In configuration 3, the ATR was modelled as an adiabatic PFR. This was done by adjusting the oxygen flow rate into the ATR so that the outlet temperature of the reactor is kept constant at 1030 °C. This was made possible by using the adjust block on Aspen HYSYS. The compositions of all the important streams and the reactor data is shown in table 6-6 and 6-7 respectively.

Table 6-6 Molar fraction data of configuration 3

	NG	TO PRE-REFORMER	OUT PRE-REFORMER	STEAM	IN ATR	Oxygen	OUT ATR
Comp Mole Frac (H_2O)	0.000	0.000	0.333	1.000	0.333	0.000	0.000
Comp Mole Frac (Oxygen)	0.000	0.000	0.000	0.000	0.000	1.000	0.000
Comp Mole Frac (Methane)	0.950	0.950	0.611	0.000	0.611	0.000	0.000
Comp Mole Frac (Ethane)	0.020	0.020	0.000	0.000	0.000	0.000	0.000
Comp Mole Frac (Propane)	0.015	0.015	0.000	0.000	0.000	0.000	0.000
Comp Mole Frac (i-Butane)	0.010	0.010	0.000	0.000	0.000	0.000	0.000
Comp Mole Frac (i-Pentane)	0.005	0.005	0.003	0.000	0.003	0.000	0.001
Comp Mole Frac (CO)	0.000	0.000	0.000	0.000	0.000	0.000	0.113
Comp Mole Frac (Hydrogen)	0.000	0.000	0.033	0.000	0.033	0.000	0.715

Table 6-7: ATR (Adiabatic PFR) data

ATR (Adiabatic PFR)		
Vessel Temperature	1030	°C
Vessel Pressure	2800	kPa
Vapor Molar Flow	3.12E+04	kgmole/h
Act.% Conversion_1	1.6E+05	
Act.% Conversion_2	73.90	
Act.% Conversion _3	26.08	

Case 2: Staging of ATR with dossification

Study of case 2 was carried out to see the effect of staging of ATR with H_2 dossification on overall conversion and H_2:CO ratio. The flowsheet simulated in Aspen HYSYS can be seen in figure 5-4. The result of the simulation can be seen in this section. Table 6-8 shows the composition of streams related to the ATR and table 6-9 specifies the data of all three reactors. In case 2, the steam:carbon ratio was decreased to 0.5 to improve the H_2:CO ratio in the produced syngas.

Table 6-8: Molar fraction data of multi stage ATR

	NG	TO PRE-REFORMER	OUT PRE-REFORMER	OUT ATR	OUT ATR 2	OUT ATR 3	IN ATR 2	IN ATR 3
Comp Mole Frac (H_2O)	0	0	0.276	0	0	0	0	0
Comp Mole Frac (Oxygen)	0	0	0.000	0.000	0.012	0.018	0.012	0.018
Comp Mole Frac (Methane)	0.95	0.95	0.664	0.000	0.000	0.000	0.000	0.000
Comp Mole Frac (Ethane)	0.02	0.02	0.000	0.000	0.000	0.000	0.000	0.000
Comp Mole Frac (Propane)	0.015	0.015	0.000	0.000	0.000	0.000	0.000	0.000
Comp Mole Frac (i-Butane)	0.01	0.01	0.000	0.000	0.000	0.000	0.000	0.000
Comp Mole Frac (i-Pentane)	0.005	0.005	0.003	0.001	0.001	0.001	0.001	0.001
Comp Mole Frac (CO)	0	0	0.000	0.152	0.150	0.149	0.150	0.149
Comp Mole Frac (Hydrogen)	0	0	0.035	0.704	0.696	0.691	0.695	0.691

Table 6-9: Multi stage ATR data

	ATR1	ATR2	ATR3
Reactor Volume	333	333	333
Bed Voidage	0.5	0.5	0.5
Act. % Conversion_1	7.20E+04	0.1893	5.95E-35
Act. % Conversion_2	73.67	1.19E-02	6.30E-35
Act. % Conversion_3	26.28	99.98	3.87E+04

The process condition and flow rates of relevant streams are shown in the following table 6-10. Process condition was kept constant for all configurations of case 1 and case 2.

Table 6-10: Process condition data of multi stage ATR simulation

	Unit	**IN ATR**	**OUT ATR**	**IN ATR 2**	**OUT ATR 2**	**IN ATR 3**	**OUT ATR 3**
Vapor Fraction		1	1	1	1	1	1
Temperature	*C*	675	1030	694	698	697	697
Pressure	*kPa*	2800	2600	2565	2465	2465	2365
Molar Flow	*kgmole/h*	34488	80271	81271	81271	81771	81771
Mass Flow	*kg/h*	581970	967169	999169	999171	1015171	1015171
Liquid Volume Flow	*m3/h*	1486	2682	2710	2710	2724	2724
Heat Flow	*kJ/h*	-3.24E+09	-3.18E+09	-4.11E+09	-4.11E+09	-4.10E+09	-4.10E+09

6.1.1 DISCUSSION OF AUTOTHERMAL REACTOR OPTIMIZATION

Case 1: Syngas production unit with different reactor types

In case 1, three configurations were proposed and simulated. The results were recorded and presented in the previous chapter. Now, the results will be compared and analyzed. The first comparison is between configuration 1(CSTR) and configuration 2(PFR). The most important parameter that will be considered is the resultant H_2:CO ratio of syngas. In configuration 1, which a CSTR was modelled as an ATR gives H_2:CO ratio of approximately 1.8 which is suitable for subsequent FT reaction. In configuration 2 however, the resultant H_2:CO ratio is 41. This result can be explained by the conversion of key reactions. Reaction 1 which corresponds to WGS reaction and reaction 2 is the methane reforming reaction while reaction 3 is the complete combustion reaction of methane.

When a PFR was used in HYSYS, the WGS reaction (reaction 1) was displaced extremely to the right hence producing a lot of CO_2 in the expense of CO. This causes a low CO mole fraction in the resultant syngas hence a higher H_2:CO ratio. Another reason is because of the lower conversion of the reforming reaction compared to configuration 1. This means that less CO is produced from CH_4. However, it can be said that this has a lower effect to the overall result. According to reaction engineering principle, PFR conversion is higher than a CSTR for the same volume of reactor for a forward reaction[29]. This could be the reason that the WGS shift reaction is displaced extremely to the right.

In configuration 3, the flowsheet simulated was similar to configuration 2 with the only difference being the PFR was modelled as an adiabatic reactor by adjusting the oxygen flow rate. The resultant syngas produced from the adiabatic PFR has a H_2:CO ratio of approximately 6. This shows that the adiabatic PFR gives a much better result compared to the isothermal PFR. The reason behind it could be the fact that WGS reaction is less displaced to the right compared to configuration 2. Methane reforming reaction conversion also shows a slight improvement. Since the adiabatic PFR consumes less oxygen, combustion reaction conversion also decreases. This means that there more methane to undergo methane reforming reaction to produce CO. Therefore, we can say that these reasons could cause the H_2:CO ratio in configuration 3 to be lower than in configuration 2. Table 6-11 summarizes the analysis of all three configurations in case 1.

Table 6-11: Summary of case study 1

	Config.1	Config.2	Config.3
H_2:CO	1.8	41	6
Act.Conversion 1 (%)	100	2.70E+05	1.60E+05
Act.Conversion 2 (%)	100	60.9	73.9
Act.Conversion 3 (%)	29.5	30.7	26.1

Case 2: Staging of ATR with dossification

Base on the result of case 1, a new proposal was made to improve the performance of the ATR which is stated in case 2. It was decided that the ATR should be modelled as a PFR instead of a CSTR even though the result shows otherwise. This is because, in reality, the contact model of the ATR is more similar to PFR than CSTR.

In case 2, multiple stage ATR was simulated in Aspen HYSYS as seen in Figure 5-4. This method was investigated to improve H_2:CO ratio of the syngas produced. A total of three ATRs modelled as PFRs were simulated and studied. Based on Table 6-8, we can conclude that staging of ATR with dossification of oxygen does not improve the H_2:CO ratio. The WGS reaction conversion decreases after each reactor but this was offset by the decreasing conversion of methane reforming reaction. Hence, the CO produced is not sufficient for a low H_2:CO syngas ratio.

It is also noticed that the syngas produced using this kinetic model is not suitable for FT reaction since its H_2:CO ratio is approximately 4.6. The improvement of H_2:CO ratio in case 2 compared to case 1 was due to the lower steam:carbon ratio used in case 2. This ratio could be lowered even more by using a lower steam:carbon ratio. However, even the lowest possible steam:carbon ratio could not produce syngas with H_2:CO ratio of 2 and low steam:carbon ratio risks soot formation. This could be due to the limitation of Aspen HYSYS simulating a complex kinetic reaction with catalyst. Another reason could be a better kinetic model is needed to simulate the reactions involved in the ATR more accurately. This is because in real life application, similar operating condition as mentioned in this study should produce syngas with H_2:CO ratio of 2 as mentioned by Rafiee et al.[30]

With a better kinetic model, future researcher could explore more ways of optimizing the ATR by using kinetic approach. A kinetic approach allows us to optimize the reactors in many different ways as compared to simulating an ideal reactor. Most published study of GTL process simulated the ATR as conversion or gibs reactor. This may be correct under certain assumption and operating condition but also may be the cause of error if the condition varies. Table 6-12 summarizes the analysis of case 2.

Table 6-12: Summary of case study 2

	ATR1	ATR2	ATR3
H_2:CO	4.6	4.6	4.6
Act.Conversion 1 (%)	7.20E+04	1.89E-01	5.95E-35
Act.Conversion 2 (%)	73.67	1.19E-02	6.30E-35
Act.Conversion 3 (%)	26.30	99.90	3.87E+04

6.2 RESULT OF FISCHER-TROPSCH REACTOR OPTIMIZATION

In section 6.2, the results of all case studies pertaining to the FTR are presented. As mentioned in chapter 5, there are 2 case studies involving FTR which are case 3 and 4. Case 3 and case 4 study the effect of void fraction in FTR and the effect of staging of FTR respectively. Table 6-11 shows the product distribution with varying void fraction.

Case 3: Influence of cobalt catalyst characteristic on product distribution

Table 6-13: Variation of molar fraction of desired product with catalyst void fraction in FTR

Name/VOID	0.1	0.2	0.3	0.4	0.5	0.6	0.7	0.8	0.9	1
Comp Mole Frac (Methane)	1.51E-2	2.64E-2	3.45E-2	4.09E-2	4.44E-2	4.75E-2	4.84E-2	5.00E-2	5.21E-2	5.52E-2
Comp Mole Frac (Ethane)	1.18E-5	1.32E-5	1.39E-5	1.47E-5	1.46E-5	1.49E-5	1.44E-5	1.45E-5	1.48E-5	1.57E-5
Comp Mole Frac (Propane)	5.98E-6	6.54E-6	8.19E-6	8.26E-6	6.95E-6	8.76E-6	7.11E-6	6.80E-6	7.65E-6	8.83E-6
Comp Mole Frac (i-Butane)	1.31E-5	1.42E-5	1.76E-5	1.78E-5	1.49E-5	1.88E-5	1.52E-5	1.45E-5	1.63E-5	1.89E-5
Comp Mole Frac (i-Pentane)	2.58E-2	2.86E-2	3.01E-2	3.16E-2	3.11E-2	3.15E-2	2.99E-2	2.99E-2	3.08E-2	3.29E-2
Comp Mole Frac (n-Hexane)	1.56E-4	1.66E-4	2.04E-4	2.05E-4	1.70E-4	2.14E-4	1.71E-4	1.64E-4	1.84E-4	2.14E-4
Comp Mole Frac (n-Heptane)	3.87E-4	4.06E-4	4.97E-4	4.97E-4	4.13E-4	5.18E-4	4.14E04	3.96E-4	4.45E-4	5.17E-4
Comp Mole Frac (n-Octane)	1.26E-3	1.31E-3	1.58E-3	1.57E-3	1.31E-3	1.63E-3	1.30E-3	1.24E-3	1.39E-3	1.61E-3
Comp Mole Frac (n-Nonane)	2.81E-3	2.86E-3	3.45E-3	3.42E-3	2.85E-3	3.54E-3	2.83E-3	2.70E-3	3.03E-3	3.50E-3
Comp Mole Frac (n-Decane)	8.40E-3	8.57E-3	1.02E-2	1.01E-2	8.43E-3	1.04E-2	8.30E-3	7.90E-3	8.84E-3	1.02E-2
Comp Mole Frac (n-C11)	1.75E-2	1.78E-2	2.07E-2	2.06E-2	1.73E-2	2.08E-2	1.67E-2	1.59E-2	1.78E-2	2.06E-2
Comp Mole Frac (n-C12)	3.82E-2	3.97E-2	4.48E-2	4.50E-2	3.84E-2	4.41E-2	3.54E-2	3.36E-2	3.75E-2	4.40E-2
Comp Mole Frac (n-C13)	7.61E-2	8.27E-2	8.84E-2	9.10E-2	7.96E-2	8.47E-2	6.78E-2	6.44E-2	7.15E-2	8.61E-2
Comp Mole Frac (n-C14)	1.10E-1	1.25E-1	1.28E-1	1.35E-1	1.20E-1	1.19E-1	9.51E-2	9.02E-2	1.00E-1	1.24E-1
Comp Mole Frac (n-C15)	8.30E-2	9.55E-2	9.49E-2	1.01E-1	9.13E-2	8.80E-2	7.00E-2	6.64E-2	7.36E-2	9.17E-2
Comp Mole Frac (n-C16)	8.79E-2	1.02E-1	1.01E-1	1.08E-1	9.79E-2	9.29E-2	7.37E-2	6.99E-2	7.76E-2	9.72E-2
Comp Mole Frac (n-C17)	8.93E-2	1.04E-1	1.02E-1	1.10E-1	9.99E-2	9.43E-2	7.49E-2	7.10E-2	7.88E-2	9.89E-2
Comp Mole Frac (n-C18)	9.01E-2	1.06E-1	1.03E-1	1.11E-1	1.01E-1	9.51E-2	7.55E-2	7.15E-2	7.94E-2	9.98E-2
Comp Mole Frac (n-C19)	9.04E-2	1.06E-1	1.04E-1	1.12E-1	1.01E-1	9.54E-2	7.57E-2	7.18E-2	7.96E-2	1.00E-1
Comp Mole Frac (n-C20)	4.62E-2	5.36E-2	5.22E-2	5.62E-2	5.10E-2	4.79E-2	3.80E-2	3.61E-2	4.00E-2	5.03E-2
Comp Mole Frac (n-C30)	1.90E-1	7.52E-2	6.10E-2	4.36E-3	9.68E-2	1.07E-1	2.72E-1	3.04E-1	2.35E-1	7.09E-2

The product was classified into three groups depending on the length of carbon chain namely $C_{5\rightarrow10}$, $C_{11\rightarrow20}$ and C_{21+}. This was done to make the analysis process easier and it is also consistent with this study's objective which is to increase molar fraction of desired product. A graph of multiple hydrocarbon products distribution variation with void fraction was plotted as shown in figure 6-1.

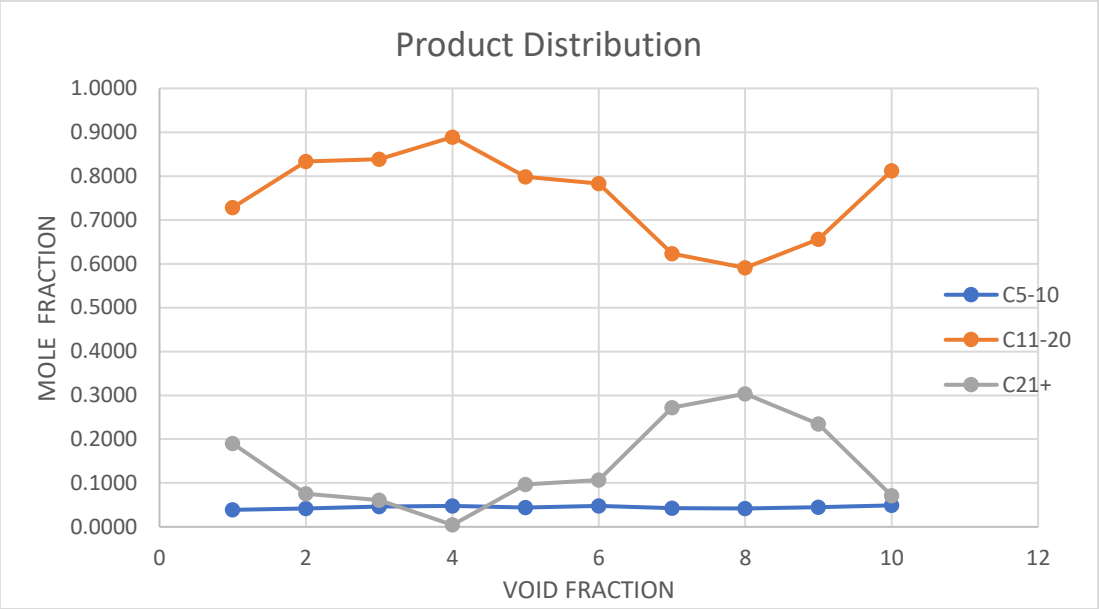

Figure 6-1: variation of molar fraction of desired product with catalyst void fraction in FTR

It was observed that among all catalyst parameters mentioned in section 5.2, only void fraction shows influence on the product distribution. Other parameters however did not give any effect. Hence, only void fraction parameter was pursued and studied. The analysis of this result will be discussed in the following part of this thesis. Table 6-14 shows the summary of the reaction data in the FTR for case 3.

Table 6-14: single stage FTR data

	FTR
Reactor Volume (m3)	2000
Bed Voidage	0.4
Act.Conversion (%)	19.65

Case 4: Effect of staging of FTR with Hydrogen dossification

The effect of staging of FTR on overall conversion and product distribution was investigated as shown in figure 5-7. In the second and third FTR, pure hydrogen was injected to maintain the H_2:CO ratio at every inlet of the FTR. The composition of the products and the reactor data are shown in table 6-15 and table 6-16 respectively. Table 6-17 shows the operation condition and molar flows of streams.

Table 6-15: Molar fraction data of multiple stage FTR simulation

	IN FTR 1	OUT FTR 1	IN FTR 2	OUT FTR 2	UNCONV. GAS	PRODUCT 2
Comp Mole Frac (H_2O)	0.000	0.034	0.033	0.061	0.002	0.001
Comp Mole Frac (Oxygen)	0.000	0.000	0.000	0.000	0.000	0.000
Comp Mole Frac (Methane)	0.003	0.037	0.037	0.064	0.068	0.008
Comp Mole Frac (Ethane)	0.000	0.000	0.000	0.000	0.000	0.000
Comp Mole Frac (Propane)	0.000	0.000	0.000	0.000	0.000	0.000
Comp Mole Frac (i-Butane)	0.000	0.000	0.000	0.000	0.000	0.000
Comp Mole Frac (i-Pentane)	0.001	0.001	0.001	0.001	0.001	0.020
Comp Mole Frac (n-Hexane)	0.000	0.000	0.000	0.000	0.000	0.000
Comp Mole Frac (n-Heptane)	0.000	0.000	0.000	0.000	0.000	0.000
Comp Mole Frac (n-Octane)	0.000	0.000	0.000	0.000	0.000	0.002
Comp Mole Frac (n-Nonane)	0.000	0.000	0.000	0.000	0.000	0.003
Comp Mole Frac (n-Decane)	0.000	0.000	0.000	0.000	0.000	0.010
Comp Mole Frac (n-C11)	0.000	0.000	0.000	0.000	0.000	0.021
Comp Mole Frac (n-C12)	0.000	0.000	0.000	0.000	0.000	0.045
Comp Mole Frac (n-C13)	0.000	0.000	0.000	0.000	0.000	0.088
Comp Mole Frac (n-C14)	0.000	0.000	0.000	0.000	0.000	0.126
Comp Mole Frac (n-C15)	0.000	0.000	0.000	0.000	0.000	0.095
Comp Mole Frac (n-C16)	0.000	0.000	0.000	0.000	0.000	0.101
Comp Mole Frac (n-C17)	0.000	0.000	0.000	0.000	0.000	0.103
Comp Mole Frac (n-C18)	0.000	0.000	0.000	0.000	0.000	0.104
Comp Mole Frac (n-C19)	0.000	0.000	0.000	0.000	0.000	0.104
Comp Mole Frac (n-C20)	0.000	0.000	0.000	0.000	0.000	0.053
Comp Mole Frac (n-C30)	0.000	0.000	0.000	0.000	0.000	0.051
Comp Mole Frac (CO)	0.293	0.279	0.273	0.261	0.278	0.015
Comp Mole Frac (Hydrogen)	0.598	0.537	0.546	0.497	0.528	0.011
Comp Mole Frac (CO_2)	0.105	0.112	0.109	0.115	0.122	0.039

Table 6-16: Reactor data of multiple stage FTR

	FTR1	FTR2
Reactor Volume (m3)	1000	1000
Heat Flow (kJ/h)	2,36E+08	1,66E+08
Bed Voidage	0.4	0.4
Act.% Conversion	11.69	9.46

Table 6-17: Process condition of multiple stage FTr simulation

	Unit	IN FTR 1	OUT FTR 1	IN FTR 2	OUT FTR 2	UNCONV. GAS	PRODUCT 2
Vapor Fraction		1	1	1	1	1	0
Temperature	*C*	210.0	220.0	210.0	220.0	30.0	30.0
Pressure	*kPa*	2465.0	2465.0	2465.0	2465.0	2465.0	2465.0
Molar Flow	*kgmole/h*	33486.7	31351.7	32001.7	30437.1	28643.5	0.3
Mass Flow	*kg/h*	473728.5	473848.3	475158.7	475186.6	442752.1	74.1
Liquid Volume Flow	*m3/h*	1118.7	1065.5	1084.3	1045.2	1012.7	0.1
Heat Flow	*kJ/h*	-2.29E+09	-2.51E+09	-2.52E+09	-2.67E+09	-2.42E+09	-1.51E+05

6.2.1 DISCUSSION OF FISCHER-TROPSCH REACTOR OPTIMIZATION

Case 3: Influence of cobalt catalyst characteristic on product distribution

In FTS, the role of the catalyst is of high importance. Carbon monoxide and hydrogen must be transported from the exterior of the catalyst to the active sites. The catalyst effectiveness as well as the selectivity of the reaction is very much dependent on the presence of both reactants in about stoichiometric amount.[3] Because of this, different catalyst parameters have been investigated to learn the effect on FT product distribution. From the simulations carried out in HYSYS, only void fraction shows an effect on the conversion and product distribution. This could be because the fact that FTS is a structure insensitive reaction by the definition of Boudart.[31], [32]

As depicted in Figure 6-1, selectivity also varies with void fraction. As mentioned in the objective of this study, the aim is to maximize hydrocarbon product of range $C_{13} - C_{19}$ which can be represented by the line $C_{11} - C_{20}$ in figure 6-1. The optimal void fraction to maximize the desired product was found to be 0.4. This means that 60% of the reactor is filled with Cobalt catalyst. We can see that selectivity towards the desired product increases steadily from 0.8 until void fraction of 0.4 baring out void fraction 1.0 and 0.9 since it is impossible to actually produce FT products without catalyst or with too small amount of catalyst. After this point, it can be seen that mole fraction of desired product decreases until void fraction 0.1.

A dimensionless parameter($\Phi = \chi^* \Psi$) was defined in Iglesia et al. [31] to explain the selectivity of Cobalt catalyst. This structural term χ contains structural catalyst properties that can be independently measured and it appears in the Φ term for all values of n.

Mole fraction of desired product increased because the selectivity towards it increases. This could be due to the effects of catalyst structure and site density suggested by the parameter χ which gives rise to an increase in the extent of readsorption and in C5+ selectivity as Co site density is increased by increasing Co loading.[31]

As seen in figure 6-1, mole fraction of desired product decreases from void fraction 0.4 to 0.1. This may be caused by the chain termination probabilities increase as χ increases above a threshold value (0.4), because diffusional restrictions inhibit chain growth steps by reducing the supply of monomer species required for chain growth.[31] Therefore, we can say that the threshold and optimal value of void fraction for the desired FT product is 0.4.

Case 4: Effect of staging of FTR with Hydrogen dossification

In case 4, the effect of staging of FTR was investigated. The proposed configuration was a simulation of a 2-stage FTR with extra feed to be distributed after the first reactor. Pure hydrogen gas was injected into the second reactor together with the outlet stream of the first reactor. The flowsheet simulated in HYSYS can be seen in Figure 5-7.

Pure hydrogen was inserted before entering the second reactor to ensure stoichiometric amount of syngas enters the following FTR. It was also observed that the consumption of reactant was not stoichiometrically equal. The FTR consumes slightly more H_2 than the stoichiometric coefficient and therefore the unreacted syngas has a higher H_2:CO ratio compared to the syngas inlet of the FTR. The reason for this could be because hydrogen adsorb easier onto the Cobalt catalyst surface compared to CO. Hence, more hydrogen gas is reacted.

We will now compare the performance of multiple stage FTR to a single stage FTR as shown in case 3. The total reactor volume of case 3 and 4 was kept constant and the operating condition was also the same in both cases. It was observed that the total conversion of FTS in a multi stage configuration was 21.15% compared to 19.65% in a single stage FTR. This shows a 7% improvement of conversion in the multi stage reactor. Resultant of the increased in conversion, the molar fraction of the desired product increased as well. The sum of molar fraction of the desired product as shown in the red box in table 6-15 shows a 23% improvement compared to a single stage FTR configuration. We can conclude that staging of FTR reactor not only increase total conversion but it also improves the product distribution by producing a higher value product range. Table 6-18 summarizes the comparison between the two configurations of FTR.

Table 6-18: Summary of multi stage FTR data

	Case 3 (Single FTR)	Case 4 (Multiple FTR)
Total Conversion (%)	19.65	21.15
Total molar fraction of desired product	0.55	0.72

6.3 RESULT OF OVERALL PROCESS OPTIMIZATION

After completing all case studies, a final proposal of GTL plant configuration was made. The final configuration was simulated and determined to be the optimal configuration. Among the key criteria of the optimal configuration is as below:

I. Optimal inlet temperature of ATR to improve H_2:CO ratio
II. Separation product and by-product after each stage of FTR
III. Single stage ATR
IV. Optimum Steam:Carbon ratio

A graph of variation of H_2:CO ratio against inlet temperature of ATR was depicted and can be seen in figure 6-2.

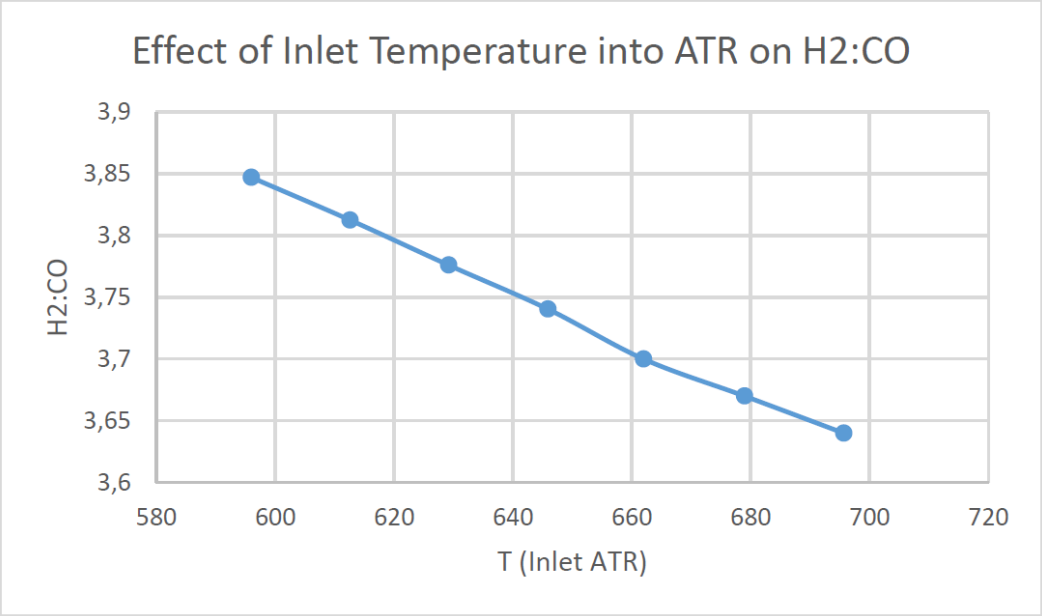

Figure 6-2: Variation of inlet temperature of ATR with H_2:CO ratio in syngas

The performance of the FT reactors was also observed. Table 6-19 shows the conversion of FTR and other reactor data.

Table 6-19: Reactor data of optimal FTR configuration

	FTR1	FTR2
Reactor Volume (m3)	1000	1000
Bed Voidage	0.4	0.4
Heat Flow (kJ/h)	2,36E+08	1,87E+08
Act.% Conversion	11.69	10.59

Lastly, it was proposed that a single stage ATR was used instead of multiple stages of ATR based on the result of previous case studies. Table 6-19 shows the H_2:CO ratio at the outlet stream of ATR.

Table 6-20: Molar fraction of optimal ATR configuration

	IN ATR	OUT ATR
Comp Mole Frac (H_2O)	0.228	0.000
Comp Mole Frac (Oxygen)	0.000	0.000
Comp Mole Frac (Methane)	0.710	0.004
Comp Mole Frac (Ethane)	0.000	0.000
Comp Mole Frac (Propane)	0.000	0.000
Comp Mole Frac (i-Butane)	0.000	0.000
Comp Mole Frac (i-Pentane)	0.003	0.001
Comp Mole Frac (CO)	0.000	0.180
Comp Mole Frac (Hydrogen)	0.036	0.694
Comp Mole Frac (CO_2)	0.022	0.121

Figure 6-3 shows the effect of steam:carbon ration on H_2:CO ratio.

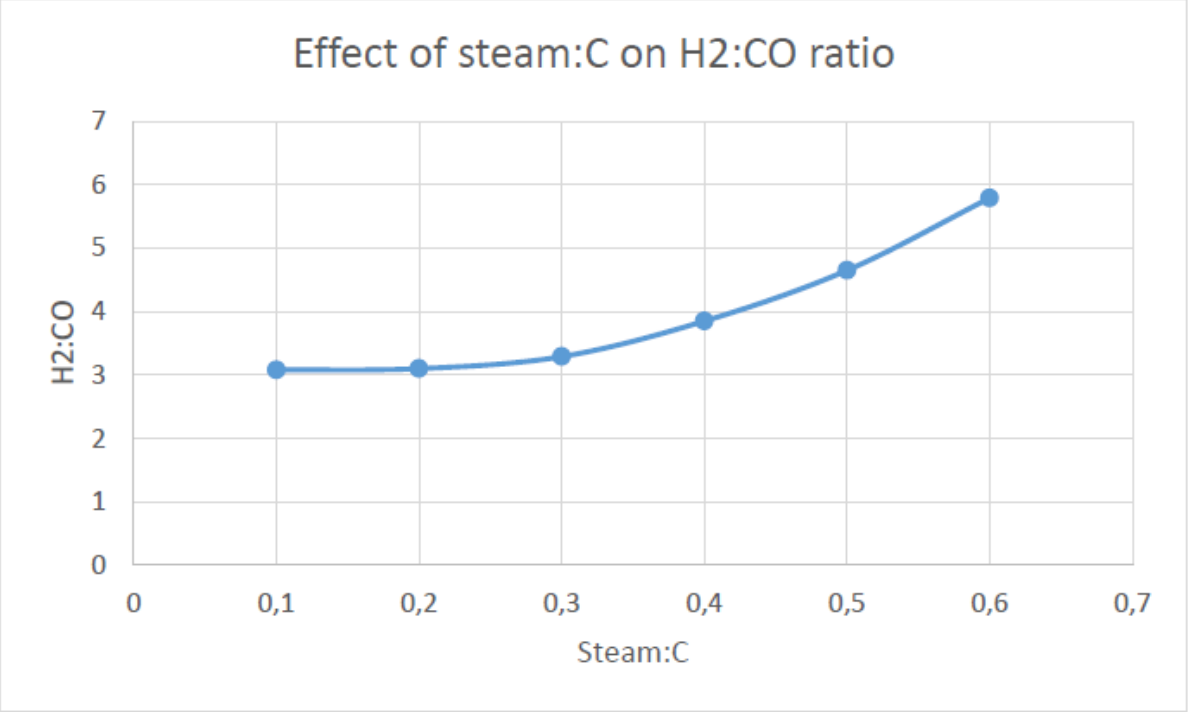

Figure 6-3: Effect of steam on H_2:CO ratio in syngas

6.3.1 DISCUSSION OF OVERALL PROCESS OPTIMIZATION

After carrying out all case studies mentioned earlier, an optimal GTL plant configuration was proposed. The final configuration of the plant took into account the optimization of the ATR, FTR, Steam:Carbon ratio in the pre-reformer as well as the inlet temperature of the ATR. The mentioned parameters play an important role in optimizing the GTL plant and must be optimized accurately.

The optimal configuration and condition of the ATR was proposed after studying case study 1 and 2. It was decided that the best configuration of ATR is a single stage reactor without any extra feed. This is because it was found out that staging of ATR reactor does not improve total conversion nor lower the H_2:CO ratio. Hence, it is more economical to have a single stage reactor without additional heaters or coolers.

Secondly, it was observed that the steam:carbon ratio in the pre-reformer affects the H_2:CO ratio in syngas produced in the ATR greatly as shown in figure 6-3. By lowering the ratio of steam:carbon, the H_2:CO ratio can be improved greatly which would be useful to use in FTS. It was decided that a steam:carbon ratio of 0.4 should be used in the pre-reformer. This ratio is ideal as it would reduce H_2:CO ratio in syngas and at the same time avoid soot formation.

Next, as shown in figure 6-2, increasing outlet temperature in ATR could lower the H_2:CO ratio in the resultant syngas. Excessive temperature however would not be possible due to material and catalyst limitation. The recommended inlet temperature of ATR was decided to be around 675 °C. This will help to produce a low H_2:CO ratio of syngas. Ideally, a better kinetic model is needed to model the reaction in the ATR to accurately optimize the reactor.

Finally, it was observed that a multiple stage FTR with product separation in between the reactors could improve the overall conversion even higher compared to the configuration mentioned in case 4 and would be the optimal configuration. The process flowsheet can be seen in figure 5-8 and the result can be seen in table 6-19 and 6-20. It can be seen that the overall conversion of the optimal configuration is 22.28% compared to 21.15% in case 4. Conversion improves 5% compared to case 4. The total reactor volume is the same for all the configurations but by removing these streams an increase in residence time occurs. Higher residence time will increase the conversion of reactants ($CO+H_2$) resulting in higher production amounts. This configuration however would involve a higher capital cost as it needs additional coolers and 3-phase separators. A cost-benefit study should be carried out to determine the preferred configuration.

Taking everything into account, a final and optimal GTL plant flow diagram has been proposed and can be seen in figure 6-4.

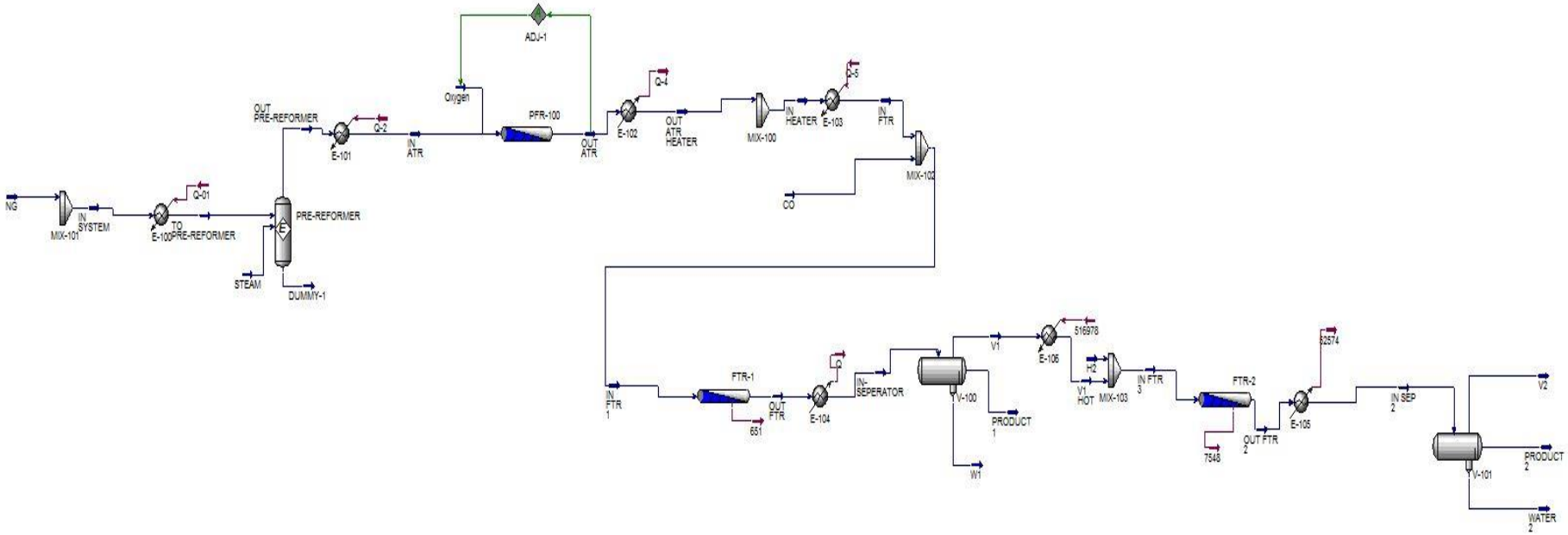

Figure 6-4: Optimal GTL plant configuration

7. CONCLUSION

A GTL Fischer-Tropsch plant was modelled and simulated using Aspen HYSYS v8.6. The impact of different parameters on the performance of syngas unit, FTS unit and the overall process was studied. A few different configurations with respect to the syngas production unit and the FTR were explored.

The syngas production unit which is the ATR was modelled as CSTR and PFR and their results were compared and analyzed. It was found that modelling the ATR as a CSTR in HYSYS would produce syngas that is suitable to be used in FTS however when using a PFR, the syngas produced has a relatively high H_2:CO ratio. The H_2:CO ratio could be reduced by modelling the PFR as an adiabatic reactor by adjusting the oxygen flow rate. Staging of ATR does not improve conversion nor lower the H_2:CO ratio. Hence, the optimal configuration of ATR with the kinetic data given in the literature would be a single stage PFR without dispersion of extra feed. A better kinetic model may be required to model accurately the complex reactions in the ATR and to be able to properly optimize the reactions.

The FTR with cobalt based catalyst was modelled as a PFR and the effect of void fraction of catalyst in FTR were considered. Optimal void fraction was recorded to be 0.4 which produced the highest molar fraction of desired product. Staging of FTR showed positive result as conversion increases 7% compared to a single stage FTR with the same total volume of reactor. Besides that, molar fraction of desired product increases by 23%. The proposed optimal configuration showed the best result by recording 5% increase in conversion compared to a multi stage FTR. The optimal configuration involves separation of product and water in between each stage of reactors. The optimal configuration would however incur a higher capital cost as additional coolers and separators are needed.

The overall process condition was also optimized and different parameters were selected to observe the impact on the overall process. Among the parameters studied were the inlet temperature of ATR and the steam:carbon ratio in the pre-reformer. The inlet temperature was varied and it was observed that syngas with lower H_2:CO ratio was produced with higher inlet temperature. Nevertheless, the maximum inlet temperature of ATR is constrained by material and catalyst limitations. Steam:carbon ratio also showed a great influence to the ratio of H_2:CO in syngas. Low steam:carbon ratio produced syngas with low H_2:CO ratio which is suitable for FTS. Soot formation however poses a risk when low steam:carbon ratio is used in the pre-reformer. Hence, it was decided that a ratio of 0.4 is optimal since low H_2:CO syngas can be produced and soot formation can be avoided. Finally, the optimum GTL FT plant after taking into account all case studies was proposed to include a single stage ATR modelled as a PFR as well as a multi stage FTR modelled as PFR with product and water separation between each stage.

BIBLIOGRAPHY

[1] A. Rafiee, "Optimal design issues of a gas-to-liquid process Optimal design issues of a gas-to-liquid process Thesis for the degree of Philosophiae Doctor Norwegian University of," no. July, 2015.

[2] K. Moen, "Modelling and Optimization of a GTL Plant," no. June, 2014.

[3] R. M. de Deugd, "Fischer-Tropsch Synthesis Revisited; Efficiency and Selectivity Benefits from Imposing Temporal and/or Spatial Structure in the Reactor," 2004.

[4] M. Panahi, A. Rafiee, S. Skogestad, and M. Hillestad, "A Natural Gas to Liquids (GTL) Process Model for Optimal Operation," *Ind. Eng. Chem. Res.*, 2011.

[5] Y. Heon, K. Jun, H. Joo, C. Han, and I. Kyu, "A simulation study on gas-to-liquid (natural gas to Fischer – Tropsch synthetic fuel) process optimization," vol. 155, pp. 427–432, 2009.

[6] I. J. Otaraku, "Technical Analysis of the Natural Gas to Hydrocarbon Liquid Process," *Am. J. Chem. Eng.*, vol. 3, no. 2, p. 25, 2017.

[7] K. Aasberg-Petersen, T. S. Christensen, C. S. Nielsen, and I. Dybkjær, "Recent developments in autothermal reforming and pre-reforming for synthesis gas production in GTL applications," *Fuel Process. Technol.*, vol. 83, no. 1-3 SPEC., pp. 253–261, 2003.

[8] G. Akinbola, "Modelling and Optimization of Urban," no. June, 2009.

[9] M. Panahi, "Optimal Design of a Gas-to-Liquids Process with a Staged Fischer-Tropsch Reactor," vol. i, no. 10, pp. 1778–1784, 2016.

[10] Y. H. Kim, H. Y. Lee, K.-W. Jun, H. Joo, C. Han, and I. K. Song, "GTL process optimization simulation study," no. 1, pp. 736/1-736/13, 2008.

[11] D. L. Hoang and S. H. Chan, "Modeling of a catalytic autothermal methane reformer for fuel cell applications," *Appl. Catal. A Gen.*, vol. 268, no. 1–2, pp. 207–216, 2004.

[12] M. E. Dry, "High quality diesel via the Fischer-Tropsch process - A review," *Journal of Chemical Technology and Biotechnology*. 2002.

[13] P. L. Spath and D. C. Dayton, "Preliminary Screening -- Technical and Economic Assessment of Synthesis Gas to Fuels and Chemicals with Emphasis on the Potential for Biomass-Derived Syngas," 2003.

[14] M. Hillestad, "Modeling the Fischer-Tropsch Product Distribution and Model Implementation," *Chem. Prod. Process Model.*, 2015.

[15] H. S. Song, D. Ramkrishn, S. Trinh, and H. Wright, "Operating strategies for Fischer-Tropsch reactors: A model-directed study," *Korean J. Chem. Eng.*, 2004.

[16] G. P. van der Laan, *PhD dissertation, Kinetics, Selectivity and Scale Up of the Fischer-Tropsch Synthesis*. 1999.

[17] A. P. Steynberg, M. E. Dry, B. H. Davis, and B. B. Breman, "Chapter 2 – Fischer-Tropsch Reactors," in *Studies in Surface Science and Catalysis*, 2004.

[18] R. Guettel, U. Kunz, and T. Turek, "Reactors for Fischer-Tropsch synthesis," *Chem. Eng. Technol.*, vol. 31, no. 5, pp. 746–754, 2008.

[19] P. K. Bakkerud, "Update on synthesis gas production for GTL," *Catal. Today*, 2005.

[20] F. Qasim, J. S. Shin, J. H. Jeong, and S. J. Park, "An Optimization Study on Syngas Production and Economic Evaluation," vol. 07001, 2016.

[21] D. J. Wilhelm, D. R. Simbeck, A. D. Karp, and R. L. Dickenson, "Syngas production for gas-to-liquids applications: Technologies, issues and outlook," *Fuel Process. Technol.*, 2001.

[22] G. F. Froment, "Methane Steam Reforming , Methanation and Water-Gas Shift : 1 . Intrinsic Kinetics," vol. 35, no. 1, pp. 88–96, 1989.

[23] A. Rafiee, "Synthesis Gas Production Configurations for Gas-to-Liquid Applications," no. 5, pp. 870–876, 2012.

[24] C. Maretto and R. Krishna, "Design and optimisation of a multi-stage bubble column slurry reactor for Fischer – Tropsch synthesis," vol. 66, pp. 241–248, 2001.

[25] A. Rafiee, "Staging of the Fischer-Tropsch Reactor with a Cobalt-Based Catalyst," no. 00, pp. 1–11, 2013.

[26] M. Hillestad, "Systematic staging in chemical reactor design," *Chem. Eng. Sci.*, 2010.

[27] E. Iglesia, "Design, synthesis, and use of cobalt-based Fischer-Tropsch synthesis catalysts," vol. 161, pp. 59–78, 1997.

[28] M. Panahi, S. Skogestad, and R. Yelchuru, "Steady State Simulation for Optimal Design and Operation of a GTL Process," in *Proceedings of the 2nd Annual Gas Processing Symposium*, 2010.

[29] O. Levenspiel, *Chemical Reaction Engineering - third edition*. 1999.

[30] A. Rafiee, "Optimal design and operation of a gas-to- liquid process," *Chem. Eng. Trans.*, vol. Volume 21, no. January, 2010.

[31] E. Iglesia, "Design, synthesis, and use of cobalt-based Fischer-Tropsch synthesis catalysts," *Design*, vol. 161, pp. 59–78, 1997.

[32] M. Boudart, "Catalysis by Supported Metals," *Adv. Catal.*, 1969.

ANNEX

Annex A: Flowsheet diagram of case study 1- Configuration 1

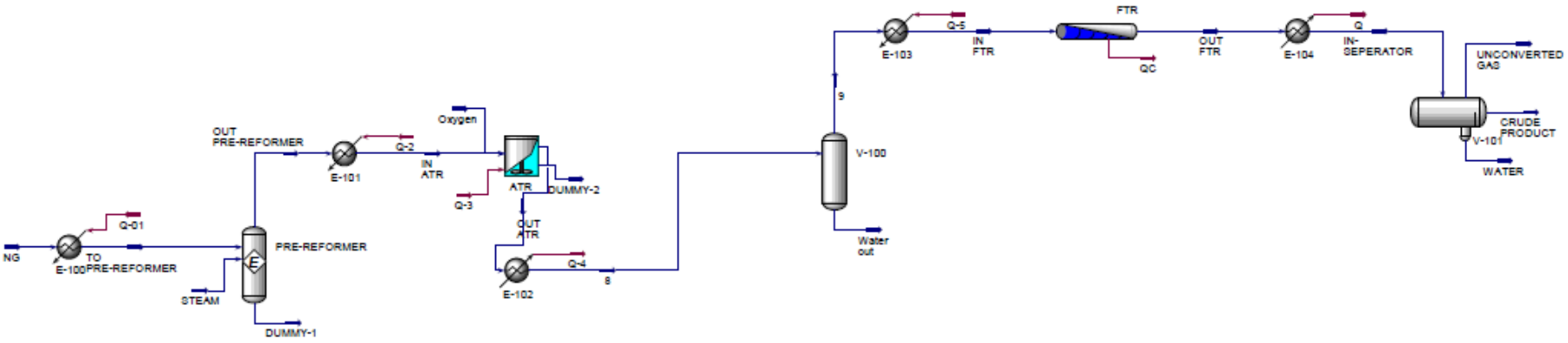

	NG	TO PRE-REFORMER	DUMMY-1	OUT PRE-REFORMER	STEAM	IN ATR	Oxygen	DUMMY-2	OUT ATR	8	9	Water out	IN FTR	OUT FTR	IN- SEPERATOR	UNCONVERTED GAS	CRUDE PRODUCT	WATER
Comp Mole Frac (H2O)	0	0	0,33296	0,332633	1	0,332633	0	0,207039	0,207041	0,207041	0,002837	0,999953	0,002837	0,224902	0,224902	0,001967	0,000585	0,999979
Comp Mole Frac (Oxygen)	0	0	0	0	0	0	1	0,006471	0,006471	0,006471	0,008137	0,000001	0,008137	0,008658	0,008658	0,011148	0,000926	0,000001
Comp Mole Frac (Methane)	0,95	0,95	0,610514	0,610826	0	0,610826	0	0,000001	0,000001	0,000001	0,000001	0	0,000001	0,285846	0,285846	0,368067	0,040909	0
Comp Mole Frac (Ethane)	0,02	0,02	0,000037	0,000037	0	0,000037	0	0,000016	0,000016	0,000016	0,000021	0	0,000021	0,000022	0,000022	0,000028	0,000015	0
Comp Mole Frac (Propane)	0,015	0,015	0	0	0	0	0	0	0	0	0	0	0	0,000004	0,000004	0,000005	0,000008	0
Comp Mole Frac (i-Butane)	0,01	0,01	0	0	0	0	0	0	0	0	0	0	0	0,000003	0,000003	0,000004	0,000018	0
Comp Mole Frac (i-Pentane)	0,005	0,005	0,002934	0,002935	0	0,002935	0	0,001313	0,001313	0,001313	0,001651	0	0,001651	0,001756	0,001756	0,002261	0,031653	0
Comp Mole Frac (n-Hexane)	0	0	0	0	0	0	0	0	0	0	0	0	0	0,000003	0,000003	0,000004	0,000209	0
Comp Mole Frac (n-Heptane)	0	0	0	0	0	0	0	0	0	0	0	0	0	0,000002	0,000002	0,000003	0,000507	0
Comp Mole Frac (n-Octane)	0	0	0	0	0	0	0	0	0	0	0	0	0	0,000002	0,000002	0,000003	0,001607	0
Comp Mole Frac (n-Decane)	0	0	0	0	0	0	0	0	0	0	0	0	0	0,000002	0,000002	0,000002	0,010302	0
Comp Mole Frac (n-C11)	0	0	0	0	0	0	0	0	0	0	0	0	0	0,000001	0,000001	0,000002	0,020967	0
Comp Mole Frac (n-C12)	0	0	0	0	0	0	0	0	0	0	0	0	0	0,000001	0,000001	0,000001	0,045594	0
Comp Mole Frac (n-C13)	0	0	0	0	0	0	0	0	0	0	0	0	0	0,000001	0,000001	0,000001	0,091657	0
Comp Mole Frac (n-C14)	0	0	0	0	0	0	0	0	0	0	0	0	0	0,000001	0,000001	0	0,134744	0
Comp Mole Frac (n-C15)	0	0	0	0	0	0	0	0	0	0	0	0	0	0,000001	0,000001	0	0,10102	0
Comp Mole Frac (n-C16)	0	0	0	0	0	0	0	0	0	0	0	0	0	0,000001	0,000001	0	0,107594	0
Comp Mole Frac (n-C17)	0	0	0	0	0	0	0	0	0	0	0	0	0	0,000001	0,000001	0	0,109648	0
Comp Mole Frac (n-C18)	0	0	0	0	0	0	0	0	0	0	0	0	0	0,000001	0,000001	0	0,110679	0
Comp Mole Frac (n-C19)	0	0	0	0	0	0	0	0	0	0	0	0	0	0,000001	0,000001	0	0,111085	0
Comp Mole Frac (n-C20)	0	0	0	0	0	0	0	0	0	0	0	0	0	0	0	0	0,055934	0
Comp Mole Frac (n-C30)	0	0	0	0	0	0	0	0	0	0	0	0	0	0	0	0	0,00426	0
Comp Mole Frac (CO)	0	0	0,000124	0,000124	0	0,000124	0	0,282164	0,282163	0,282163	0,354826	0,000019	0,354826	0,091666	0,091666	0,118031	0,006249	0,000005
Comp Mole Frac (Hydrogen)	0	0	0,033433	0,033446	0	0,033446	0	0,502996	0,502995	0,502995	0,632527	0,000027	0,632527	0,387121	0,387121	0,498469	0,010337	0,000015
Comp Mole Frac (CO2)	0	0	0,019998	0,019999	0	0,019999	0	0	0	0	0	0	0	0	0	0	0	0
Comp Mole Frac (n-Nonane)	0	0	0	0	0	0	0	0	0	0	0	0	0	0,000002	0,000002	0,000002	0,003492	0

	Unit	NG	TO PRE-REFORMER	DUMMY-1	OUT PRE-REFORMER	STEAM	IN ATR	Oxygen	DUMMY-2	OUT ATR	8	9	Water out	IN FTR	OUT FTR	IN- SEPERATOR	UNCONVERTED GAS	CRUDE PRODUCT	WATER
Vapour Fraction		1	1	0	1	1	1	1	0	1	0,795206	1	0	1	1	0,776612	1	0	0
Temperature	*C*	40	455	376,461913	376,461913	252	675	200	1030	1030	38	38	38	210	220	30	30	30	30
Pressure	*kPa*	3000	2900	2900	2900	4045	2800	3000	2800	2800	2765	2765	2765	2665	2465	2430	2430	2430	2430
Molar Flow	*kgmole/h*	8195	8195	0	13960,87867	5204	13960,87867	5236	0	31218,2186	31218,2186	24824,9	6393,318573	24824,9	23333,177	23333,177	18120,82309	0,203036	5212,150871
Mass Flow	*kg/h*	142966,717	142966,7174	0	236717,3833	93750,58289	236717,3833	167552	0	404270,8547	404270,8547	289096,107	115174,7481	289096,107	289189,0632	289189,0632	195250,4228	42,190893	93896,44953
Liquid Volume Flow	*m3/h*	454,942076	454,942076	0	573,988573	93,939775	573,988573	147,27515	0	888,94919	888,94919	773,53649	115,4127	773,53649	798,332116	798,332116	704,18895	0,054924	94,088241
Heat Flow	*kJ/h*	-627173957	-449480204,5	0	-1677180833	-1227700592	-1449025500	26985789,1	0	-1520123595	-2812616042	-989539653	-1823076389	-863734586	-1861922661	-2240093237	-750445401,6	-84069,5027	-1489563766

Annex B: Case study 1- Configuration 2

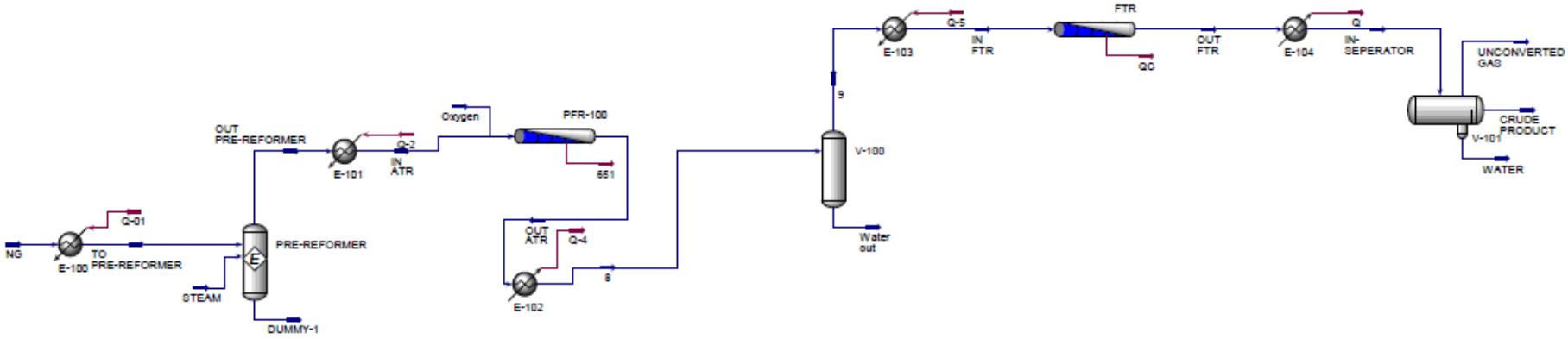

Column1	NG	TO PRE-REFORMER	DUMMY-1	OUT PRE-REFORMER	STEAM	IN ATR	Oxygen	OUT ATR	8	9	Water out	IN FTR	OUT FTR	IN- SEPERATOR	UNCONVERTED GAS	CRUDE PRODUCT	WATER
Comp Mole Frac (H2O)	0	0	0.33296	0.332633	1	0.332633	0	0	0	0	0	0	0.065873	0.065873	0.002206	0.000602	0.998326
Comp Mole Frac (Oxygen)	0	0	0	0	0	0	1	0.000007	0.000007	0.000007	0.000007	0.000007	0.000007	0.000007	0.000008	0.000001	0
Comp Mole Frac (Methane)	0.95	0.95	0.610514	0.610826	0	0.610826	0	0.000044	0.000044	0.000044	0.000044	0.000044	0.084907	0.084907	0.090705	0.009254	0
Comp Mole Frac (Ethane)	0.02	0.02	0.000037	0.000037	0	0.000037	0	0.000016	0.000016	0.000016	0.000016	0.000016	0.000017	0.000017	0.000018	0.000009	0
Comp Mole Frac (Propane)	0.015	0.015	0	0	0	0	0	0	0	0	0	0	0.000004	0.000004	0.000004	0.000006	0
Comp Mole Frac (i-Butane)	0.01	0.01	0	0	0	0	0	0	0	0	0	0	0.000003	0.000003	0.000003	0.000013	0
Comp Mole Frac (i-Pentane)	0.005	0.005	0.002934	0.002935	0	0.002935	0	0.001321	0.001321	0.001321	0.001321	0.001321	0.001346	0.001346	0.001438	0.019036	0
Comp Mole Frac (n-Hexane)	0	0	0	0	0	0	0	0	0	0	0	0	0.000003	0.000003	0.000003	0.000153	0
Comp Mole Frac (n-Heptane)	0	0	0	0	0	0	0	0	0	0	0	0	0.000002	0.000002	0.000002	0.00037	0
Comp Mole Frac (n-Octane)	0	0	0	0	0	0	0	0	0	0	0	0	0.000002	0.000002	0.000002	0.001188	0
Comp Mole Frac (n-Decane)	0	0	0	0	0	0	0	0	0	0	0	0	0.000002	0.000002	0.000002	0.007868	0
Comp Mole Frac (n-C11)	0	0	0	0	0	0	0	0	0	0	0	0	0.000001	0.000001	0.000001	0.016464	0
Comp Mole Frac (n-C12)	0	0	0	0	0	0	0	0	0	0	0	0	0.000001	0.000001	0.000001	0.037404	0
Comp Mole Frac (n-C13)	0	0	0	0	0	0	0	0	0	0	0	0	0.000001	0.000001	0.000001	0.080394	0
Comp Mole Frac (n-C14)	0	0	0	0	0	0	0	0	0	0	0	0	0.000001	0.000001	0	0.125737	0
Comp Mole Frac (n-C15)	0	0	0	0	0	0	0	0	0	0	0	0	0.000001	0.000001	0	0.096318	0
Comp Mole Frac (n-C16)	0	0	0	0	0	0	0	0	0	0	0	0	0.000001	0.000001	0	0.103933	0
Comp Mole Frac (n-C17)	0	0	0	0	0	0	0	0	0	0	0	0	0.000001	0.000001	0	0.106353	0
Comp Mole Frac (n-C18)	0	0	0	0	0	0	0	0	0	0	0	0	0.000001	0.000001	0	0.10755	0
Comp Mole Frac (n-C19)	0	0	0	0	0	0	0	0	0	0	0	0	0.000001	0.000001	0	0.108017	0
Comp Mole Frac (n-C20)	0	0	0	0	0	0	0	0	0	0	0	0	0	0	0	0.054313	0
Comp Mole Frac (n-C30)	0	0	0	0	0	0	0	0	0	0	0	0	0	0	0	0.053396	0
Comp Mole Frac (CO)	0	0	0.000124	0.000124	0	0.000124	0	0.113275	0.113275	0.113275	0.113276	0.113275	0.030561	0.030561	0.032647	0.001594	0.000001
Comp Mole Frac (Hydrogen)	0	0	0.033433	0.033446	0	0.033446	0	0.714632	0.714632	0.714632	0.714625	0.714632	0.64332	0.64332	0.68725	0.01307	0.00002
Comp Mole Frac (CO2)	0	0	0.019998	0.019999	0	0.019999	0	0.170704	0.170704	0.170704	0.170711	0.170704	0.173941	0.173941	0.185706	0.054334	0.001653
Comp Mole Frac (n-Nonane)	0	0	0	0	0	0	0	0	0	0	0	0	0.000002	0.000002	0.000002	0.002623	0

Column1	*Unit*	NG	TO PRE-REFORMER	DUMMY-1	OUT PRE-REFORMER	STEAM	IN ATR	Oxygen	OUT ATR	8	9	Water out	IN FTR	OUT FTR	IN- SEPERATOR	UNCONVERTED GAS	CRUDE PRODUCT	WATER
apour Fraction		1	1	0	1	1	1	1	1	1	1	0	1	1	0.936077	1	0	0
Temperature	*C*	40	455	376.461913	376.461913	252	675	200	1030.010013	38	38	38	210	220	30	30	30	30
Pressure	*kPa*	3000	2900	2900	2900	4045	2800	3000	2600	2565	2565	2565	2465	2265	2230	2230	2230	2230
Molar Flow	*kgmole/h*	8195	8195	0	13960.87867	5204	13960.87867	4448.93429	31013.72061	31013.72061	31013.72061	0	31013.72061	30436.60803	30436.60803	28491.01223	0.249253	1945.34654
Mass Flow	*kg/h*	142966.717	142966.7174	0	236717.3833	93750.58289	236717.3833	142365.897	379081.4978	379081.4978	379081.4978	0	379081.4978	379197.9797	379197.9797	344014.984	54.389125	35128.6066
uid Volume F	*m3/h*	454.942076	454.942076	0	573.988573	93.939775	573.988573	125.137025	1049.860869	1049.860869	1049.860869	0	1049.860869	1059.574556	1059.574556	1024.274287	0.070066	35.230203
Heat Flow	*kJ/h*	-627173957	-449480204.5	0	-1677180833	-1227700592	-1449025500	22929335.8	-1426131875	-2470180947	-2470180947	0	-2302443179	-2681842201	-2956436325	-2400004656	-111642.2	-556320027

Annex C: Case study 1 – Configuration 3

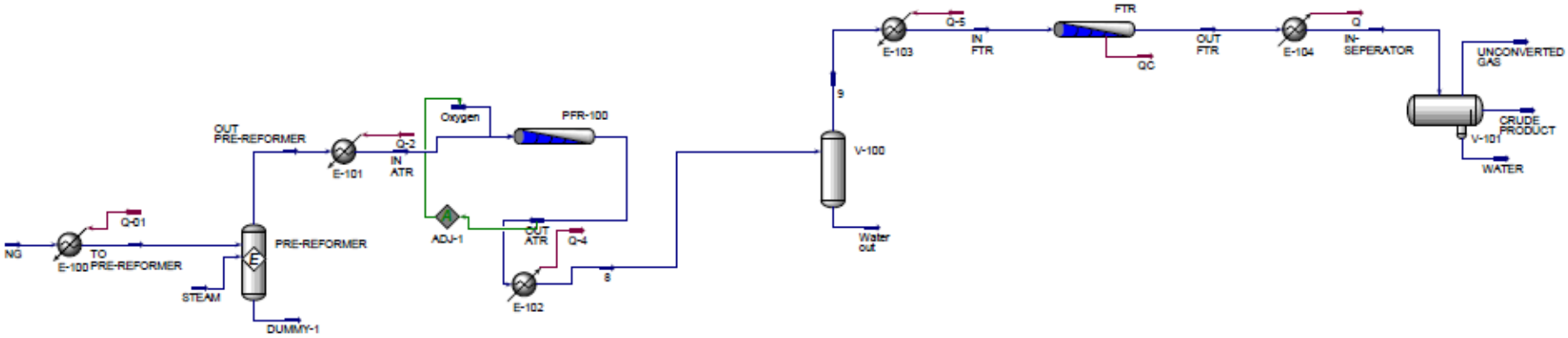

Column1	NG	TO PRE-REFORMER	DUMMY-1	OUT PRE-REFORMER	STEAM	IN ATR	Oxygen	OUT ATR	8	9	Water out	IN FTR	OUT FTR	IN- SEPERATOR	UNCONVERTED GAS	CRUDE PRODUCT	WATER
Comp Mole Frac (H2O)	0	0	0.33296	0.332633	1	0.332633	0	0	0	0	0	0	0.065874	0.065874	0.002206	0.000603	0.998326
Comp Mole Frac (Oxygen)	0	0	0	0	0	0	1	0.000008	0.000008	0.000008	0.000008	0.000008	0.000008	0.000008	0.000008	0.000001	0
Comp Mole Frac (Methane)	0.95	0.95	0.610514	0.610826	0	0.610826	0	0.000041	0.000041	0.000041	0.000041	0.000041	0.084905	0.084905	0.090703	0.009364	0
Comp Mole Frac (Ethane)	0.02	0.02	0.000037	0.000037	0	0.000037	0	0.000016	0.000016	0.000016	0.000016	0.000016	0.000017	0.000017	0.000018	0.000009	0
Comp Mole Frac (Propane)	0.015	0.015	0	0	0	0	0	0	0	0	0	0	0.000004	0.000004	0.000004	0.000006	0
Comp Mole Frac (i-Butane)	0.01	0.01	0	0	0	0	0	0	0	0	0	0	0.000003	0.000003	0.000003	0.000013	0
Comp Mole Frac (i-Pentane)	0.005	0.005	0.002934	0.002935	0	0.002935	0	0.001321	0.001321	0.001321	0.001321	0.001321	0.001346	0.001346	0.001438	0.019409	0
Comp Mole Frac (n-Hexane)	0	0	0	0	0	0	0	0	0	0	0	0	0.000003	0.000003	0.000003	0.000156	0
Comp Mole Frac (n-Heptane)	0	0	0	0	0	0	0	0	0	0	0	0	0.000002	0.000002	0.000002	0.000378	0
Comp Mole Frac (n-Octane)	0	0	0	0	0	0	0	0	0	0	0	0	0.000002	0.000002	0.000002	0.001213	0
Comp Mole Frac (n-Decane)	0	0	0	0	0	0	0	0	0	0	0	0	0.000002	0.000002	0.000002	0.008028	0
Comp Mole Frac (n-C11)	0	0	0	0	0	0	0	0	0	0	0	0	0.000001	0.000001	0.000001	0.01682	0
Comp Mole Frac (n-C12)	0	0	0	0	0	0	0	0	0	0	0	0	0.000001	0.000001	0.000001	0.038382	0
Comp Mole Frac (n-C13)	0	0	0	0	0	0	0	0	0	0	0	0	0.000001	0.000001	0.000001	0.083401	0
Comp Mole Frac (n-C14)	0	0	0	0	0	0	0	0	0	0	0	0	0.000001	0.000001	0	0.132223	0
Comp Mole Frac (n-C15)	0	0	0	0	0	0	0	0	0	0	0	0	0.000001	0.000001	0	0.101877	0
Comp Mole Frac (n-C16)	0	0	0	0	0	0	0	0	0	0	0	0	0.000001	0.000001	0	0.110349	0
Comp Mole Frac (n-C17)	0	0	0	0	0	0	0	0	0	0	0	0	0.000001	0.000001	0	0.11306	0
Comp Mole Frac (n-C18)	0	0	0	0	0	0	0	0	0	0	0	0	0.000001	0.000001	0	0.114408	0
Comp Mole Frac (n-C19)	0	0	0	0	0	0	0	0	0	0	0	0	0.000001	0.000001	0	0.114936	0
Comp Mole Frac (n-C20)	0	0	0	0	0	0	0	0	0	0	0	0	0	0	0	0.057803	0
Comp Mole Frac (n-C30)	0	0	0	0	0	0	0	0	0	0	0	0	0	0	0	0.005756	0
Comp Mole Frac (CO)	0	0	0.000124	0.000124	0	0.000124	0	0.113276	0.113276	0.113276	0.113277	0.113276	0.030561	0.030561	0.032648	0.001598	0.000001
Comp Mole Frac (Hydrogen)	0	0	0.033433	0.033446	0	0.033446	0	0.714634	0.714634	0.714634	0.714626	0.714634	0.643321	0.643321	0.687251	0.013111	0.00002
Comp Mole Frac (CO2)	0	0	0.019998	0.019999	0	0.019999	0	0.170703	0.170703	0.170703	0.17071	0.170703	0.17394	0.17394	0.185705	0.054417	0.001653
Comp Mole Frac (n-Nonane)	0	0	0	0	0	0	0	0	0	0	0	0	0.000002	0.000002	0.000002	0.002678	0

Column1	*Unit*	NG	TO PRE-REFORMER	DUMMY-1	OUT PRE-REFORMER	STEAM	IN ATR	Oxygen	OUT ATR	8	9	Water out	IN FTR	OUT FTR	IN- SEPERATOR	UNCONVERTED GAS	CRUDE PRODUCT	WATER
Vapour Fraction		1	1	0	1	1	1	1	1	1	1	0	1	1	0.936077	1	0	0
Temperature	*C*	40	455	376.461913	376.461913	252	675	200	1030.004485	38	38	38	210	220	30	30	30	30
Pressure	*kPa*	3000	2900	2900	2900	4045	2800	3000	2600	2565	2565	2565	2465	2265	2230	2230	2230	2230
Molar Flow	*kgmole/h*	8195	8195	0	13960.87867	5204	13960.87867	4448.98368	31013.94173	31013.94173	31013.94173	0	31013.94173	30436.80946	30436.80946	28491.19314	0.234879	1945.38144
Mass Flow	*kg/h*	142966.717	142966.7174	0	236717.3833	93750.58289	236717.3833	142367.478	379083.7276	379083.7276	379083.7276	0	379083.7276	379195.4806	379195.4806	344017.1469	49.09714	35129.2366
Liquid Volume Flow	*m3/h*	454.942076	454.942076	0	573.988573	93.939775	573.988573	125.138414	1049.86626	1049.86626	1049.86626	0	1049.86626	1059.574344	1059.574344	1024.279993	0.063515	35.230835
Heat Flow	*kJ/h*	-627173957	-449480204.5	0	-1677180833	-1227700592	-1449025500	22929590.4	-1426142399	-2470189906	-2470189906	0	-2302451150	-2681851680	-2956444682	-2400013396	-101278.9371	-556330007

Annex D: Case study 2

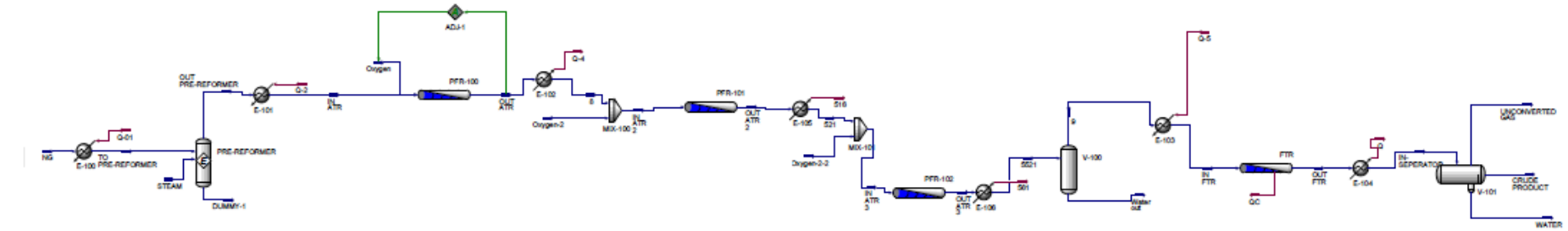

Column1	NG	TO PRE-REFORMER	DUMMY-1	STEAM	OUT ATR	8	9	Water out	IN FTR	OUT FTR	IN- SEPERATOR	UNCONVERTED GAS	CRUDE PRODUCT	WATER	OUT ATR 2	521	IN ATR 2	OUT PRE-REFORMER	IN ATR	Oxygen	Oxygen-2	Oxygen-2-2	IN ATR 3	OUT ATR 3	5521
Comp Mole Frac (H2O)	0	0	0.276241	1	0	0	0	0	0	0.040663	0.040663	0.00239	0.000599	0.998774	0	0	0	0.27599	0.27599	0	0	0	0	0	0
Comp Mole Frac (Oxygen)	0	0	0	0	0.000009	0.000009	0.018075	0.018075	0.018075	0.018287	0.018287	0.019017	0.001339	0.000001	0.012034	0.012034	0.012314	0	0	1	1	1	0.018075	0.018075	0.018075
Comp Mole Frac (Methane)	0.95	0.95	0.663826	0	0.000142	0.000142	0	0	0	0.052384	0.052384	0.054477	0.005151	0	0	0	0.00014	0.664068	0.664068	0	0	0	0	0	0
Comp Mole Frac (Ethane)	0.02	0.02	0.00005	0	0.000022	0.000022	0.000021	0.000021	0.000021	0.000021	0.000021	0.000022	0.00001	0	0.000021	0.000021	0.000021	0.00005	0.00005	0	0	0	0.000021	0.000021	0.000021
Comp Mole Frac (Propane)	0.015	0.015	0	0	0	0	0	0	0	0.000004	0.000004	0.000004	0.000006	0	0	0	0	0	0	0	0	0	0	0	0
Comp Mole Frac (i-Butane)	0.01	0.01	0	0	0	0	0	0	0	0.000003	0.000003	0.000003	0.000012	0	0	0	0	0	0	0	0	0	0	0	0
Comp Mole Frac (i-Pentane)	0.005	0.005	0.003189	0	0.00137	0.00137	0.001345	0.001345	0.001345	0.001361	0.001361	0.001415	0.017896	0	0.001353	0.001353	0.001353	0.00319	0.00319	0	0	0	0.001345	0.001345	0.001345
Comp Mole Frac (n-Hexane)	0	0	0	0	0	0	0	0	0	0.000003	0.000003	0.000003	0.000148	0	0	0	0	0	0	0	0	0	0	0	0
Comp Mole Frac (n-Heptane)	0	0	0	0	0	0	0	0	0	0.000002	0.000002	0.000002	0.000362	0	0	0	0	0	0	0	0	0	0	0	0
Comp Mole Frac (n-Octane)	0	0	0	0	0	0	0	0	0	0.000002	0.000002	0.000002	0.001168	0	0	0	0	0	0	0	0	0	0	0	0
Comp Mole Frac (n-Decane)	0	0	0	0	0	0	0	0	0	0.000002	0.000002	0.000002	0.007819	0	0	0	0	0	0	0	0	0	0	0	0
Comp Mole Frac (n-C11)	0	0	0	0	0	0	0	0	0	0.000001	0.000001	0.000001	0.016507	0	0	0	0	0	0	0	0	0	0	0	0
Comp Mole Frac (n-C12)	0	0	0	0	0	0	0	0	0	0.000001	0.000001	0.000001	0.038019	0	0	0	0	0	0	0	0	0	0	0	0
Comp Mole Frac (n-C13)	0	0	0	0	0	0	0	0	0	0.000001	0.000001	0.000001	0.083849	0	0	0	0	0	0	0	0	0	0	0	0
Comp Mole Frac (n-C14)	0	0	0	0	0	0	0	0	0	0.000001	0.000001	0	0.134414	0	0	0	0	0	0	0	0	0	0	0	0
Comp Mole Frac (n-C15)	0	0	0	0	0	0	0	0	0	0.000001	0.000001	0	0.103979	0	0	0	0	0	0	0	0	0	0	0	0
Comp Mole Frac (n-C16)	0	0	0	0	0	0	0	0	0	0.000001	0.000001	0	0.112831	0	0	0	0	0	0	0	0	0	0	0	0
Comp Mole Frac (n-C17)	0	0	0	0	0	0	0	0	0	0.000001	0.000001	0	0.115651	0	0	0	0	0	0	0	0	0	0	0	0
Comp Mole Frac (n-C18)	0	0	0	0	0	0	0	0	0	0.000001	0.000001	0	0.117046	0	0	0	0	0	0	0	0	0	0	0	0
Comp Mole Frac (n-C19)	0	0	0	0	0	0	0	0	0	0.000001	0.000001	0	0.117588	0	0	0	0	0	0	0	0	0	0	0	0
Comp Mole Frac (n-C20)	0	0	0	0	0	0	0	0	0	0	0	0	0.059154	0	0	0	0	0	0	0	0	0	0	0	0
Comp Mole Frac (n-C30)	0	0	0	0	0	0	0	0	0	0	0	0	0.007836	0	0	0	0	0	0	0	0	0	0	0	0
Comp Mole Frac (CO)	0	0	0.000189	0	0.151942	0.151942	0.148876	0.148877	0.148876	0.098232	0.098232	0.102157	0.00457	0.000003	0.149792	0.149792	0.150073	0.000189	0.000189	0	0	0	0.148876	0.148876	0.148876
Comp Mole Frac (Hydrogen)	0	0	0.035119	0	0.704015	0.704015	0.691379	0.691376	0.691379	0.647079	0.647079	0.672932	0.011678	0.000017	0.695633	0.695633	0.695353	0.035128	0.035128	0	0	0	0.691379	0.691379	0.691379
Comp Mole Frac (CO2)	0	0	0.021387	0	0.142499	0.142499	0.140303	0.140306	0.140303	0.141944	0.141944	0.147567	0.039782	0.001204	0.141166	0.141166	0.140746	0.021386	0.021386	0	0	0	0.140303	0.140303	0.140303
Comp Mole Frac (n-Nonane)	0	0	0	0	0	0	0	0	0	0.000002	0.000002	0.000002	0.002586	0	0	0	0	0	0	0	0	0	0	0	0

Column1	*Unit*	NG	TO PRE-REFORMER	DUMMY-1	STEAM	OUT ATR	8	9	Water out	IN FTR	OUT FTR	IN- SEPERATOR	UNCONVERTED GAS	CRUDE PRODUCT	WATER	OUT ATR 2	521	IN ATR 2	OUT PRE-REFORMER	IN ATR	Oxygen	Oxygen-2	Oxygen-2-2	IN ATR 3	OUT ATR 3	5521
Vapour Fraction		1	1	0	1	1	1	1	0	1	1	0.961581	1	0	0	1	1	1	1	1	1	1	1	1	1	1
Temperature	*C*	40	455	387.533737	252	1029.983868	700	38	38	210	220	30	30	30	30	697.605655	700	694.067106	387.533737	675	200	200	200	697.052805	697.054321	38
Pressure	*kPa*	3000	2900	2900	4045	2600	2565	2365	2365	2265	2065	2030	2030	2030	2030	2465	2465	2565	2900	2800	3000	3000	3000	2465	2365	2365
Molar Flow	*kgmole/h*	22000	22000	0	11000	80271.08476	80271.08476	81771.22174	0	81771.22174	80826.09573	80826.09573	77720.82529	0.628881	3104.64157	81271.22174	81271.22174	81271.08476	34488.1329	34488.1329	12037.617	1000	500	81771.22174	81771.22174	81771.22174
Mass Flow	*kg/h*	383803.2683	383803.2683	0	198166.1053	967169.3451	967169.3451	1015171.209	0	1015171.209	1015477.738	1015477.738	959316.933	133.931317	56026.874	999171.2093	999171.2093	999169.3451	581969.5863	581969.5863	385203.743	32000	16000	1015171.209	1015171.209	1015171.209
Liquid Volume Flow	*m3/h*	1221.32101	1221.32101	0	198.566013	2681.655244	2681.655244	2724.281164	0	2724.281164	2740.366435	2740.366435	2684.017422	0.173086	56.175927	2710.217456	2710.217456	2709.78266	1486.434875	1486.434875	338.587058	28.127416	14.063708	2724.281164	2724.281164	2724.281164
Heat Flow	*kJ/h*	-1683688476	-1206658267	0	-2595062742	-3182056774	-4117420714	-5855352888	0	-5418290073	-6030609265	-6656185063	-5768208811	-273017.1674	-887703234	-4112399735	-4105691523	-4112266820	-3801720827	-3244003819	62040602.1	5153894.02	2576947.01	-4103114576	-4103214685	-5855352888

Annex E: Case study 3

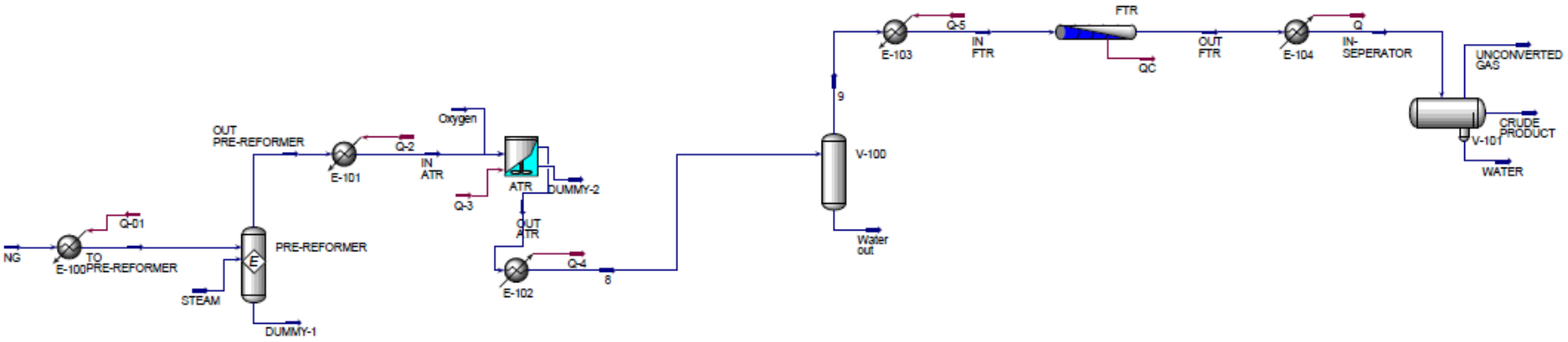

	NG	TO PRE-REFORMER	DUMMY-1	STEAM	OUT ATR	IN FTR	OUT FTR 1	OUT PRE-REFORMER	IN ATR	Oxygen	IN FTR 1	OUT ATR HEATER	IN HEATER	IN SYSTEM	CO	INLET ATR	TO SEPARATOR	UNREACTED GAS	CRUDE PROD	WATER
Comp Mole Frac (H2O)	0	0	0.227817	1	0	0	0.065012	0.227632	0.227632	0	0	0	0	0	0	0.165978	0.065012	0.001949	0.000594	0.998663
Comp Mole Frac (Oxygen)	0	0	0	0	0	0	0	0	0	1	0	0	0	0	0	0.270849	0	0	0	0
Comp Mole Frac (Methane)	0.95	0.95	0.71	0	0.003503	0.003503	0.068427	0.710181	0.710181	0	0.003022	0.003503	0.003503	0.95	0	0.517829	0.068427	0.07305	0.008337	0
Comp Mole Frac (Ethane)	0.02	0.02	0.000066	0	0.000028	0.000028	0.000027	0.000066	0.000066	0	0.000024	0.000028	0.000028	0.02	0	0.000048	0.000027	0.000029	0.000015	0
Comp Mole Frac (Propane)	0.015	0.015	0	0	0	0	0.000003	0	0	0	0	0	0	0.015	0	0	0.000003	0.000003	0.000006	0
Comp Mole Frac (i-Butane)	0.01	0.01	0	0	0	0	0.000003	0	0	0	0	0	0	0.01	0	0	0.000003	0.000003	0.000012	0
Comp Mole Frac (i-Pentane)	0.005	0.005	0.003409	0	0.001418	0.001418	0.001383	0.003409	0.003409	0	0.001224	0.001418	0.001418	0.005	0	0.002486	0.001383	0.001476	0.020027	0
Comp Mole Frac (n-Hexane)	0	0	0	0	0	0	0.000002	0	0	0	0	0	0	0	0	0	0.000002	0.000003	0.000138	0
Comp Mole Frac (n-Heptane)	0	0	0	0	0	0	0.000002	0	0	0	0	0	0	0	0	0	0.000002	0.000002	0.000337	0
Comp Mole Frac (n-Octane)	0	0	0	0	0	0	0.000002	0	0	0	0	0	0	0	0	0	0.000002	0.000002	0.001089	0
Comp Mole Frac (n-Decane)	0	0	0	0	0	0	0.000002	0	0	0	0	0	0	0	0	0	0.000002	0.000002	0.007041	0
Comp Mole Frac (n-C11)	0	0	0	0	0	0	0.000001	0	0	0	0	0	0	0	0	0	0.000001	0.000001	0.014434	0
Comp Mole Frac (n-C12)	0	0	0	0	0	0	0.000001	0	0	0	0	0	0	0	0	0	0.000001	0.000001	0.03122	0
Comp Mole Frac (n-C13)	0	0	0	0	0	0	0.000001	0	0	0	0	0	0	0	0	0	0.000001	0.000001	0.061876	0
Comp Mole Frac (n-C14)	0	0	0	0	0	0	0.000001	0	0	0	0	0	0	0	0	0	0.000001	0	0.089432	0
Comp Mole Frac (n-C15)	0	0	0	0	0	0	0.000001	0	0	0	0	0	0	0	0	0	0.000001	0	0.06772	0
Comp Mole Frac (n-C16)	0	0	0	0	0	0	0.000001	0	0	0	0	0	0	0	0	0	0.000001	0	0.071813	0
Comp Mole Frac (n-C17)	0	0	0	0	0	0	0.000001	0	0	0	0	0	0	0	0	0	0.000001	0	0.073087	0
Comp Mole Frac (n-C18)	0	0	0	0	0	0	0.000001	0	0	0	0	0	0	0	0	0	0.000001	0	0.073715	0
Comp Mole Frac (n-C19)	0	0	0	0	0	0	0.000001	0	0	0	0	0	0	0	0	0	0.000001	0	0.073959	0
Comp Mole Frac (n-C20)	0	0	0	0	0	0	0	0	0	0	0	0	0	0	0	0	0	0	0.037857	0
Comp Mole Frac (n-C30)	0	0	0	0	0	0	0.000003	0	0	0	0	0	0	0	0	0	0.000003	0	0.294634	0
Comp Mole Frac (CO)	0	0	0.000271	0	0.180254	0.180254	0.26592	0.000271	0.000271	0	0.292861	0.180254	0.180254	0	1	0.000197	0.26592	0.283884	0.016228	0.000012
Comp Mole Frac (Hydrogen)	0	0	0.036012	0	0.693637	0.693637	0.4811	0.036018	0.036018	0	0.598353	0.693637	0.693637	0	0	0.026263	0.4811	0.513601	0.011491	0.000018
Comp Mole Frac (CO2)	0	0	0.022424	0	0.121159	0.121159	0.118102	0.022422	0.022422	0	0.104516	0.121159	0.121159	0	0	0.016349	0.118102	0.125992	0.042562	0.001307
Comp Mole Frac (n-Nonane)	0	0	0	0	0	0	0.000002	0	0	0	0	0	0	0	0	0	0.000002	0.000002	0.002375	0

Column1	*Unit*	NG	TO PRE-REFORMER	DUMMY-1	STEAM	OUT ATR	IN FTR	OUT FTR 1	OUT PRE-REFORMER	IN ATR	Oxygen	IN FTR 1	OUT ATR HEATER	IN HEATER	IN SYSTEM	CO	INLET ATR	TO SEPARATOR	UNREACTED GAS	CRUDE PROD	WATER
Vapour Fraction		1	1	0	1	1	1	1	1	1	1	1	1	1	1	1	1	0.936718	1	0	0
Temperature	*C*	40	455	397.161071	252	1029.999606	210	220	397.161071	675	200	209.983729	38	38	40	210	596.028745	30	30	30	30
Pressure	*kPa*	3000	2900	2900	4045	2665	2665	2665	2900	2800	3000	2665	2665	2665	3000	2665	2800	2665	2665	2665	2665
Molar Flow	*kgmole/h*	8195	8195	0	3278	28886.64785	28886.64785	29634.32088	12018.47155	12018.47155	4464.35817	33486.64785	28886.64785	28886.64785	8195	4600	16482.82971	29634.32088	27758.98795	0.342099	1874.99083
Mass Flow	*kg/h*	142966.717	142966.7174	0	59053.4994	344878.2339	344878.2339	473870.403	202020.2953	202020.2953	142859.461	473728.3762	344878.2339	344878.2339	142966.7174	128850.142	344879.7567	473870.403	439938.4237	90.398303	33841.581
Liquid Volume Flow	*m3/h*	454.942076	454.942076	0	59.172672	957.536722	957.536722	1022.627366	538.530366	538.530366	125.570859	1118.722707	957.536722	957.536722	454.942076	161.185985	664.101225	1022.627366	988.579348	0.114484	33.933534
Heat Flow	*kJ/h*	-627173957	-449480204.5	0	-773328697	-1007543592	-1805446156	-2693027947	-1222808899	-1030487273	23008828.9	-2289393412	-1958979256	-1958979256	-627173957.2	-483947256	-1007478444	-2956027070	-2419735198	-180936.0013	-536110936

Annex F: Case study 4

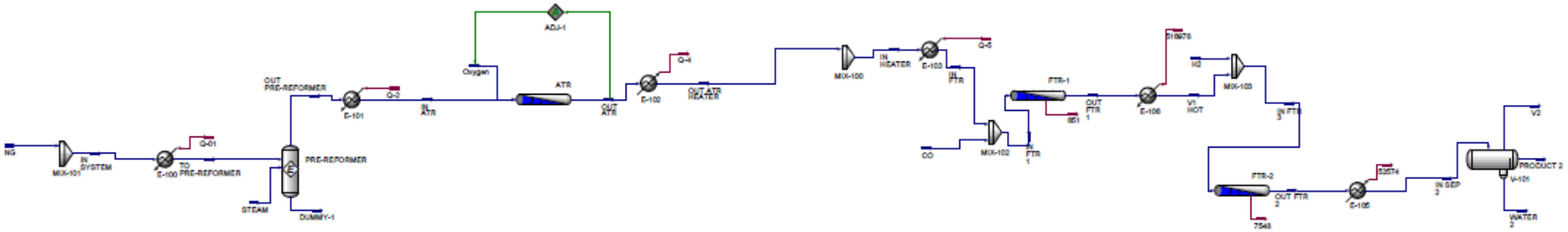

Column1	NG	TO PRE-REFORMER	DUMMY-1	STEAM	OUT ATR	IN FTR	OUT FTR 1	OUT PRE-REFORMER	IN ATR	Oxygen	IN FTR 1	OUT ATR HEATER	IN HEATER	IN SYSTEM	CO	H2	IN FTR 3	OUT FTR 2	IN SEP 2	V2	PRODUCT 2	WATER 2	V1 HOT
Comp Mole Frac (H2O)	0	0	0.227817	1	0	0	0.036756	0.227632	0.227632	0	0	0	0	0	0	0	0.036005	0.06508	0.06508	0.00207	0.000599	0.998777	0.036756
Comp Mole Frac (Oxygen)	0	0	0	0	0	0	0	0	0	1	0	0	0	0	0	0	0	0	0	0	0	0	0
Comp Mole Frac (Methane)	0.95	0.95	0.71	0	0.003507	0.003507	0.040003	0.710181	0.710181	0	0.003025	0.003507	0.003507	0.95	0	0	0.039187	0.068434	0.068434	0.073053	0.008204	0	0.040003
Comp Mole Frac (Ethane)	0.02	0.02	0.000066	0	0.000028	0.000028	0.000026	0.000066	0.000066	0	0.000024	0.000028	0.000028	0.02	0	0	0.000025	0.000026	0.000026	0.000028	0.000015	0	0.000026
Comp Mole Frac (Propane)	0.015	0.015	0	0	0	0	0.000003	0	0	0	0	0	0	0.015	0	0	0.000003	0.000004	0.000004	0.000004	0.000008	0	0.000003
Comp Mole Frac (i-Butane)	0.01	0.01	0	0	0	0	0.000003	0	0	0	0	0	0	0.01	0	0	0.000003	0.000004	0.000004	0.000004	0.000017	0	0.000003
Comp Mole Frac (i-Pentane)	0.005	0.005	0.003409	0	0.001418	0.001418	0.001314	0.003409	0.003409	0	0.001224	0.001418	0.001418	0.005	0	0	0.001287	0.001357	0.001357	0.001448	0.020568	0	0.001314
Comp Mole Frac (n-Hexane)	0	0	0	0	0	0	0.000002	0	0	0	0	0	0	0	0	0	0.000002	0.000003	0.000003	0.000003	0.000198	0	0.000002
Comp Mole Frac (n-Heptane)	0	0	0	0	0	0	0.000002	0	0	0	0	0	0	0	0	0	0.000002	0.000003	0.000003	0.000003	0.000487	0	0.000002
Comp Mole Frac (n-Octane)	0	0	0	0	0	0	0.000002	0	0	0	0	0	0	0	0	0	0.000002	0.000003	0.000003	0.000003	0.001567	0	0.000002
Comp Mole Frac (n-Decane)	0	0	0	0	0	0	0.000002	0	0	0	0	0	0	0	0	0	0.000002	0.000002	0.000002	0.000002	0.010162	0	0.000002
Comp Mole Frac (n-C11)	0	0	0	0	0	0	0.000001	0	0	0	0	0	0	0	0	0	0.000001	0.000002	0.000002	0.000002	0.02084	0	0.000001
Comp Mole Frac (n-C12)	0	0	0	0	0	0	0.000001	0	0	0	0	0	0	0	0	0	0.000001	0.000002	0.000002	0.000001	0.044996	0	0.000001
Comp Mole Frac (n-C13)	0	0	0	0	0	0	0.000001	0	0	0	0	0	0	0	0	0	0.000001	0.000002	0.000002	0.000001	0.088996	0	0.000001
Comp Mole Frac (n-C14)	0	0	0	0	0	0	0.000001	0	0	0	0	0	0	0	0	0	0.000001	0.000002	0.000002	0	0.128806	0	0.000001
Comp Mole Frac (n-C15)	0	0	0	0	0	0	0.000001	0	0	0	0	0	0	0	0	0	0.000001	0.000001	0.000001	0	0.097649	0	0.000001
Comp Mole Frac (n-C16)	0	0	0	0	0	0	0.000001	0	0	0	0	0	0	0	0	0	0.000001	0.000001	0.000001	0	0.103609	0	0.000001
Comp Mole Frac (n-C17)	0	0	0	0	0	0	0.000001	0	0	0	0	0	0	0	0	0	0.000001	0.000001	0.000001	0	0.105469	0	0.000001
Comp Mole Frac (n-C18)	0	0	0	0	0	0	0.000001	0	0	0	0	0	0	0	0	0	0.000001	0.000001	0.000001	0	0.106395	0	0.000001
Comp Mole Frac (n-C19)	0	0	0	0	0	0	0.000001	0	0	0	0	0	0	0	0	0	0.000001	0.000001	0.000001	0	0.106759	0	0.000001
Comp Mole Frac (n-C20)	0	0	0	0	0	0	0	0	0	0	0	0	0	0	0	0	0	0.000001	0.000001	0	0.054692	0	0
Comp Mole Frac (n-C30)	0	0	0	0	0	0	0	0	0	0	0	0	0	0	0	0	0	0	0	0	0.031345	0	0
Comp Mole Frac (CO)	0	0	0.000271	0	0.18025	0.18025	0.277623	0.000271	0.000271	0	0.292858	0.18025	0.18025	0	1	0	0.271956	0.259585	0.259585	0.277105	0.014861	0.000011	0.277623
Comp Mole Frac (Hydrogen)	0	0	0.036012	0	0.693634	0.693634	0.532053	0.036018	0.036018	0	0.598351	0.693634	0.693634	0	0	1	0.541605	0.489615	0.489615	0.522661	0.010959	0.000016	0.532053
Comp Mole Frac (CO2)	0	0	0.022424	0	0.121162	0.121162	0.112199	0.022422	0.022422	0	0.104519	0.121162	0.121162	0	0	0	0.109909	0.11587	0.11587	0.12361	0.039366	0.001196	0.112199
Comp Mole Frac (n-Nonane)	0	0	0	0	0	0	0.000002	0	0	0	0	0	0	0	0	0	0.000002	0.000002	0.000002	0.000002	0.003435	0	0.000002

Column1	*Unit*	NG	TO PRE-REFORMER	DUMMY-1	STEAM	OUT ATR	IN FTR	OUT FTR 1	OUT PRE-REFORMER	IN ATR	Oxygen	IN FTR 1	OUT ATR HEATER	IN HEATER	IN SYSTEM	CO	H2	IN FTR 3	OUT FTR 2	IN SEP 2	V2	PRODUCT 2	WATER 2	V1 HOT
Vapour Fraction		1	1	0	1	1	1	1	1	1	1	1	1	1	1	1	1	1	1	0.936771	1	0	0	1
Temperature	*C*	40	455	397.161071	252	1030.018216	210	220	397.161071	675	200	209.983731	38	38	40	210	210	209.97923	220	30	30	30	30	210
Pressure	*kPa*	3000	2900	2900	4045	2665	2665	2665	2900	2800	3000	2665	2665	2665	3000	2665	2665	2665	2665	2465	2465	2465	2465	2665
Molar Flow	*kgmole/h*	8195	8195	0	3278	28886.42378	28886.42378	31194.13721	12018.47155	12018.47155	4464.35817	33486.42378	28886.42378	28886.42378	8195	4600	650	31844.13721	30205.87912	30205.87912	28295.9878	0.328221	1909.5631	31194.13721
Mass Flow	*kg/h*	142966.717	142966.7174	0	59053.4994	344877.7577	344877.7577	473843.4261	202020.2953	202020.2953	142859.461	473727.9	344877.7577	344877.7577	142966.7174	128850.142	1310.40002	475153.8262	475180.8594	475180.8594	440650.974	69.852516	34460.0329	473843.4261
Liquid Volume Flow	*m3/h*	454.942076	454.942076	0	59.172672	957.533421	957.533421	1061.576872	538.530366	538.530366	125.570859	1118.719406	957.533421	957.533421	454.942076	161.185985	18.757757	1080.334628	1039.429092	1039.429092	1004.787237	0.090224	34.551631	1061.576872
Heat Flow	*kJ/h*	-627173957	-449480204.5	0	-773328697	-1007543827	-1805463998	-2525398177	-1222808899	-1030487273	23008828.9	-2289411254	-1958996347	-1958996347	-627173957.2	-483947256	3457086.97	-2532010005	-2697806943	-2965288806	-2419166556	-142522.178	-545979727	-2535467092

Annex G: Final Configuration

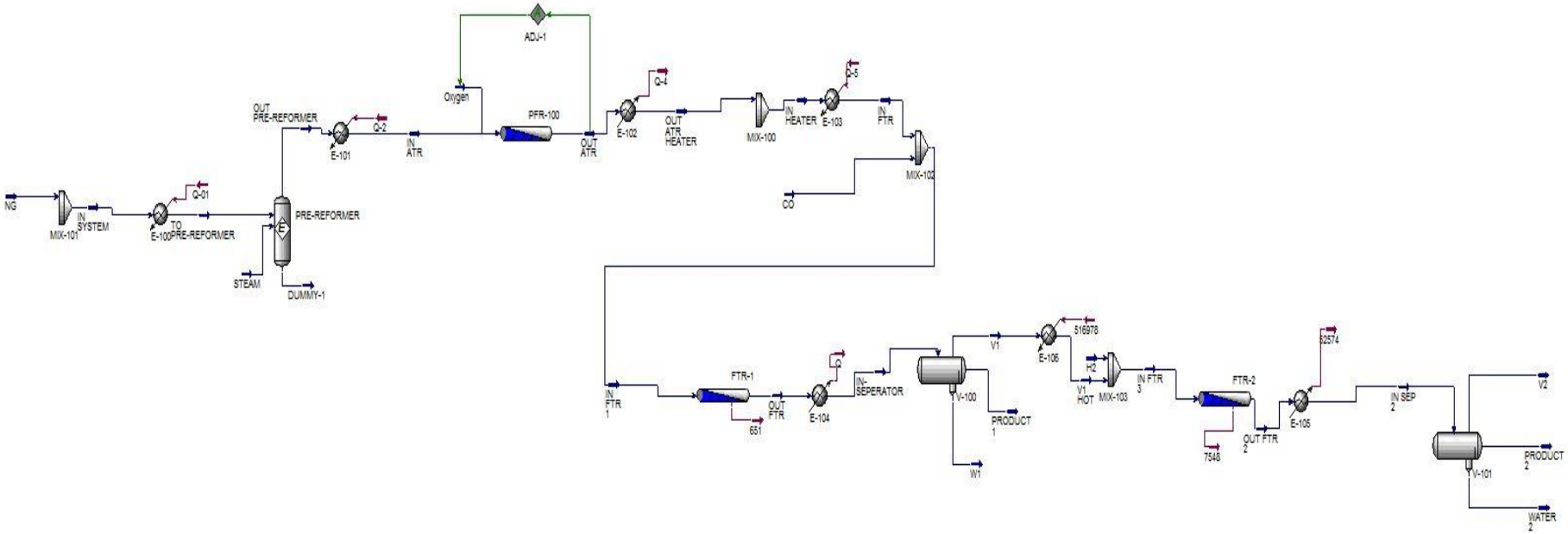

	NG	TO PRE-REFORMER	DUMMY-1	STEAM	OUT ATR	IN FTR	OUT FTR	IN- SEPERATOR	OUT PRE-REFORMER	IN ATR	Oxygen	IN FTR 1	OUT ATR HEATER	IN HEATER	IN SYSTEM	CO	H2	IN FTR 3	OUT FTR 2	IN SEP 2	V2	PRODUCT 2	WATER 2	V1	PRODUCT 1	W1	V1 HOT
Comp Mole Frac (H2O)	0	0	0.227817	1	0	0	0.036756	0.036756	0.227632	0.227632	0	0	0	0	0	0	0	0.001903	0.033736	0.033736	0.00207	0.0006	0.998765	0.001944	0.000598	0.998758	0.001944
Comp Mole Frac (Oxygen)	0	0	0	0	0	0	0	0	0	0	1	0	0	0	0	0	0	0	0	0	0	0	0	0	0	0	0
Comp Mole Frac (Methane)	0.95	0.95	0.71	0	0.003507	0.003507	0.040003	0.040003	0.710181	0.710181	0	0.003025	0.003507	0.003507	0.95	0	0	0.040575	0.07486	0.07486	0.077317	0.008752	0	0.041451	0.004973	0	0.041451
Comp Mole Frac (Ethane)	0.02	0.02	0.000066	0	0.000028	0.000028	0.000026	0.000026	0.000066	0.000066	0	0.000024	0.000028	0.000028	0.02	0	0	0.000026	0.000028	0.000028	0.000028	0.000015	0	0.000027	0.000015	0	0.000027
Comp Mole Frac (Propane)	0.015	0.015	0	0	0	0	0.000003	0.000003	0	0	0	0	0	0	0.015	0	0	0.000003	0.000004	0.000004	0.000004	0.000008	0	0.000003	0.000006	0	0.000003
Comp Mole Frac (i-Butane)	0.01	0.01	0	0	0	0	0.000003	0.000003	0	0	0	0	0	0	0.01	0	0	0.000003	0.000004	0.000004	0.000004	0.000017	0	0.000003	0.000013	0	0.000003
Comp Mole Frac (i-Pentane)	0.005	0.005	0.003409	0	0.001418	0.001418	0.001314	0.001314	0.003409	0.003409	0	0.001224	0.001418	0.001418	0.005	0	0	0.001332	0.001417	0.001417	0.001463	0.020992	0	0.001361	0.020399	0	0.001361
Comp Mole Frac (n-Hexane)	0	0	0	0	0	0	0.000003	0.000003	0	0	0	0	0	0	0	0	0	0.000003	0.000003	0.000003	0.000003	0.000199	0	0.000003	0.000157	0	0.000003
Comp Mole Frac (n-Heptane)	0	0	0	0	0	0	0.000002	0.000002	0	0	0	0	0	0	0	0	0	0.000002	0.000003	0.000003	0.000003	0.000491	0	0.000002	0.000384	0	0.000002
Comp Mole Frac (n-Octane)	0	0	0	0	0	0	0.000002	0.000002	0	0	0	0	0	0	0	0	0	0.000002	0.000003	0.000003	0.000003	0.001577	0	0.000002	0.001246	0	0.000002
Comp Mole Frac (n-Decane)	0	0	0	0	0	0	0.000002	0.000002	0	0	0	0	0	0	0	0	0	0.000002	0.000002	0.000002	0.000002	0.010175	0	0.000002	0.008147	0	0.000002
Comp Mole Frac (n-C11)	0	0	0	0	0	0	0.000001	0.000001	0	0	0	0	0	0	0	0	0	0.000001	0.000002	0.000002	0.000002	0.020716	0	0.000001	0.016995	0	0.000001
Comp Mole Frac (n-C12)	0	0	0	0	0	0	0.000001	0.000001	0	0	0	0	0	0	0	0	0	0.000001	0.000002	0.000002	0.000001	0.044246	0	0.000001	0.037961	0	0.000001
Comp Mole Frac (n-C13)	0	0	0	0	0	0	0.000001	0.000001	0	0	0	0	0	0	0	0	0	0.000001	0.000001	0.000001	0.000001	0.08756	0	0.000001	0.079823	0	0.000001
Comp Mole Frac (n-C14)	0	0	0	0	0	0	0.000001	0.000001	0	0	0	0	0	0	0	0	0	0	0.000001	0.000001	0	0.130702	0	0	0.122593	0	0
Comp Mole Frac (n-C15)	0	0	0	0	0	0	0.000001	0.000001	0	0	0	0	0	0	0	0	0	0	0.000001	0.000001	0	0.101155	0	0	0.095171	0	0
Comp Mole Frac (n-C16)	0	0	0	0	0	0	0.000001	0.000001	0	0	0	0	0	0	0	0	0	0	0.000001	0.000001	0	0.108834	0	0	0.102382	0	0
Comp Mole Frac (n-C17)	0	0	0	0	0	0	0.000001	0.000001	0	0	0	0	0	0	0	0	0	0	0.000001	0.000001	0	0.111311	0	0	0.104675	0	0
Comp Mole Frac (n-C18)	0	0	0	0	0	0	0.000001	0.000001	0	0	0	0	0	0	0	0	0	0	0.000001	0.000001	0	0.112562	0	0	0.105821	0	0
Comp Mole Frac (n-C19)	0	0	0	0	0	0	0.000001	0.000001	0	0	0	0	0	0	0	0	0	0	0.000001	0.000001	0	0.113057	0	0	0.106271	0	0
Comp Mole Frac (n-C20)	0	0	0	0	0	0	0	0	0	0	0	0	0	0	0	0	0	0	0	0	0	0.058007	0	0	0.05451	0	0
Comp Mole Frac (n-C30)	0	0	0	0	0	0	0.000001	0.000001	0	0	0	0	0	0	0	0	0	0	0	0	0	0	0	0	0.066255	0	0
Comp Mole Frac (CO)	0	0	0.000271	0	0.18025	0.18025	0.277623	0.277623	0.000271	0.000271	0	0.292858	0.18025	0.18025	0	1	0	0.281591	0.267736	0.267736	0.276522	0.014867	0.000011	0.287671	0.016631	0.000013	0.287671
Comp Mole Frac (Hydrogen)	0	0	0.036012	0	0.693634	0.693634	0.532053	0.532053	0.036018	0.036018	0	0.598351	0.693634	0.693634	0	0	1	0.560793	0.501218	0.501218	0.517668	0.010894	0.000016	0.55131	0.01247	0.000019	0.55131
Comp Mole Frac (CO2)	0	0	0.022424	0	0.121162	0.121162	0.112199	0.112199	0.022422	0.022422	0	0.104519	0.121162	0.121162	0	0	0	0.11376	0.120974	0.120974	0.124904	0.039807	0.001208	0.116216	0.03977	0.00121	0.116216
Comp Mole Frac (n-Nonane)	0	0	0	0	0	0	0.000002	0.000002	0	0	0	0	0	0	0	0	0	0.000002	0.000002	0.000002	0.000002	0.003455	0	0.000002	0.002733	0	0.000002

Column1	Unit	NG	TO PRE-REFORMER	DUMMY-1	STEAM	OUT ATR	IN FTR	OUT FTR	IN- SEPERATOR	OUT PRE-REFORMER	IN ATR	Oxygen	IN FTR 1	OUT ATR HEATER	IN HEATER	IN SYSTEM	CO	H2	IN FTR 3	OUT FTR 2	IN SEP 2	V2	PRODUCT 2	WATER 2	V1	PRODUCT 1	W1	V1 HOT
Vapour Fraction		1	1	0	1	1	1	1	0.965068	1	1	1	1	1	1	1	1	1	1	1	0.968222	1	0	0	1	0	0	1
Temperature	C	40	455	397.161071	252	1030.018216	210	220	30	397.161071	675	200	209.983731	38	38	40	210	210	209.984855	220	30	30	30	30	30	30	30	30	210
Pressure	kPa	3000	2900	2900	4045	2665	2665	2665	2665	2900	2800	3000	2665	2665	2665	3000	2665	2665	2665	2665	2465	2465	2465	2465	2665	2665	2665	2665
Molar Flow	kgmole/h	8195	8195	0	3278	28886.42378	28886.42378	31194.14717	31194.14717	12018.47155	12018.47155	4464.35817	33486.42378	28886.42378	28886.42378	8195	4600	650	30754.4825	28920.54974	28920.54974	28001.50568	0.233751	918.810302	30104.4825	0.264829	1089.39984	30104.4825
Mass Flow	kg/h	142966.717	142966.7174	0	59053.4994	344877.7577	344877.7577	473846.6382	473846.6382	202020.2953	202020.2953	142859.461	473727.9	344877.7577	344877.7577	142966.7174	128850.142	1310.40002	455438.7496	455497.9346	455497.9346	438868.3512	48.416339	16581.1671	454128.3496	58.557541	19659.731	454128.3496
Liquid Volume Flow	m3/h	454.942076	454.942076	0	59.172672	957.533421	957.533421	1061.580891	1061.580891	538.530366	538.530366	125.570859	1118.719406	957.533421	957.533421	454.942076	161.185985	18.757757	1060.551103	1014.793764	1014.793764	998.105722	0.062703	16.625339	1041.793346	0.075333	19.712212	1041.793346
Heat Flow	kJ/h	-627173957	-449480204.5	0	-773328697	-1007543827	-1805463998	-2525401688	-2760187549	-1222808899	-1030487273	23008828.9	-2289411254	-1958996347	-1958996347	-627173957.2	-483947256	3457086.97	-2274521293	-2461767671	-2678337926	-2415532531	-99100.32425	-262706295	-2448591789	-118976.5325	-311476784	-2277978380